Non-contact surface wave measurements on pavements

Henrik Bjurström

Doctoral Thesis
KTH Royal Institute of Technology
School of Architecture and the Built Environment
Department of Civil and Architectural Engineering
Division of Soil and Rock Mechanics
SE-114 28 Stockholm, Sweden

TRITA-JOB PHD 1025
ISSN 1650-9501
ISBN 978-91-7729-263-0

Stockholm 2017

Akademisk avhandling som med tillstånd av KTH i Stockholm framlägges till offentlig granskning för avläggande av teknisk doktorsexamen onsdagen den 8 mars kl. 10.00 i Kollegiesalen, KTH, Brinellvägen 8, Stockholm.

Abstract

In this thesis, nondestructive surface wave measurements are presented for characterization of dynamic modulus and layer thickness on different pavements and cement concrete slabs. Air-coupled microphones enable rapid data acquisition without physical contact with the pavement surface.

Quality control of asphalt concrete pavements is crucial to verify the specified properties and to prevent premature failure. Testing today is primarily based on destructive testing and the evaluation of core samples to verify the degree of compaction through determination of density and air void content. However, mechanical properties are generally not evaluated since conventional testing is time-consuming, expensive, and complicated to perform. Recent developments demonstrate the ability to accurately determine the complex modulus as a function of loading time (frequency) and temperature using seismic laboratory testing. Therefore, there is an increasing interest for faster, continuous field data evaluation methods that can be linked to the results obtained in the laboratory, for future quality control of pavements based on mechanical properties.

Surface wave data acquisition using accelerometers has successfully been used to determine dynamic modulus and thickness of the top asphalt concrete layer in the field. However, accelerometers require a new setup for each individual measurement and are therefore slow when testing is performed in multiple positions. Non-contact sensors, such as air-coupled microphones, are in this thesis established to enable faster surface wave testing performed on-the-fly.

For this project, a new data acquisition system is designed and built to enable rapid surface wave measurements while rolling a data acquisition trolley. A series of 48 air-coupled micro-electro-mechanical sensor (MEMS) microphones are mounted on a straight array to realize instant collection of multichannel data records from a single impact. The data acquisition and evaluation is shown to provide robust, high resolution results comparable to conventional accelerometer measurements. The importance of a perfect alignment between the tested structure's surface and the microphone array is investigated by numerical analyses.

Evaluated multichannel measurements collected in the field are compared to resonance testing on core specimens extracted from the same positions, indicating small differences. Rolling surface wave measurements obtained in the field at different temperatures also demonstrate the strong temperature dependency of asphalt concrete.

A new innovative method is also presented to determine the thickness of plate like structures. The Impact Echo (IE) method, commonly applied to determine thickness of cement concrete slabs using an accelerometer, is not ideal when air-coupled microphones are employed due to low signal-to-noise ratio. Instead, it is established how non-contact receivers are able to identify the frequency of propagating waves with counter-directed phase velocity and group velocity, directly linked to the IE thickness resonance frequency.

The presented non-contact surface wave testing indicates good potential for future rolling quality control of asphalt concrete pavements.

Keywords

Seismic testing; asphalt concrete; dynamic modulus; non-contact measurements; rolling measurements; surface waves; Lamb waves; MEMS microphones

Sammanfattning

I denna avhandling presenteras oförstörande ytvågsmätningar för karakterisering av dynamisk modul samt lagertjocklek på olika asfaltsytor och betongplattor. Användandet av mikrofoner möjliggör snabb datainsamling utan fysisk kontakt med asfaltsytan.

Kvalitetskontroll av vägens beläggning är viktig för att verifiera att rätt egenskaper uppnåtts och för att förhindra tidiga skador och brott. Dagens kvalitetskontroll är i första hand baserad på förstörande provning och utvärdering av provkroppar där packningsgraden bestäms genom mätning av densitet och hålrumshalt. Mekaniska egenskaper bestäms dock generellt inte då konventionella testmetoder är tidskrävande, dyra och komplicerade att utföra. Ny utveckling har visat på möjligheten att på ett korrekt sätt kunna bestämma den komplexa modulen som en funktion av belastningstid (frekvens) och temperatur genom att utföra seismiska laboratoriemätningar. Därför finns nu ett ökat intresse för snabbare, kontinuerliga fältmätningsmetoder där resultaten kan länkas samman med resultat från laboratoriet för framtida kvalitetskontroll baserad på mekaniska egenskaper.

Insamling av ytvågsdata i fält med hjälp av accelerometrar har med gott resultat kunnat utföras för bestämning av dynamisk modul och lagertjocklek för det översta asfaltslagret i vägar. Accelerometer-mätningar kräver dock en ny uppställning av utrustningen för varje ny position som testas och är därför långsamma vid storskaliga tester. Det demonstreras i denna avhandling hur kontaktlösa sensorer, såsom mikrofoner, möjliggör snabbare ytvågsmätningar som utförs i rörelse.

Ett nytt datainsamlingssystem har konstruerats och byggts i detta projekt för att möjliggöra snabba rullande ytvågsmätningar. En serie om 48 mikroelektromekaniska (MEMS) mikrofoner monteras på rad för att möjliggöra flerkanalig datainsamling från en enskild impuls. Resultaten visar hur datainsamlingen och databearbetningen levererar robusta, högupplösta resultat som är jämförbara med dem från accelerometer-mätningar. Betydelsen av ett konstant avstånd mellan asfaltsytan och varje mikrofon undersöks genom numerisk analys.

Resultat från fältdata som jämförs med resonansmätningar, utförda på provkroppar som borrats från samma positioner där fältmätningarna utförts, visar små skillnader. Rullande ytvågsmätningar som genomförts i

fält vid olika temperaturer visar också på asfaltens kraftiga temperaturberoende.

En ny innovativ metod för att bestämma tjockleken på betongplattor presenteras också. Impact Echo, en metod som vanligen används för att bestämma tjocklek på betongplattor med hjälp av en accelerometer, är inte optimal när mikrofoner används på grund av deras låga signal-brusförhållande. Istället demonstreras hur kontaktlösa sensorer kan identifiera frekvensen hos propagerande vågor, med motriktad fashastighet och grupphastighet, som är direkt kopplad till tjockleks-resonansen.

De presenterade kontaktlösa ytvågsmätningarna tyder på god potential för framtida rullande kvalitetskontroll av asfaltsytor.

Nyckelord

Seismisk fältmätning; asfalt; dynamisk modul; kontaktlösa mätningar; rullande mätningar; ytvågor; Lamb-vågor; MEMS-mikrofoner

Preface

The work of the presented thesis has been carried out at the divisions of Highway and Railway Engineering, and Soil and Rock Mechanics at KTH Royal Institute of Technology in Stockholm, Sweden.

I would first like to express my sincere gratitude to my main supervisor Nils Ryden for all the support and help I have gotten during these years. Thanks also to my assisting supervisor Björn Birgisson for initiating this project and for his guidance during the work. Johan Silfwerbrand is gratefully acknowledged for the final review of this thesis.

I am very grateful towards the Swedish Transport Administration (Traikverket) and the Swedish construction industry's organization for research and development (SBUF) for their financial support.

Special thanks go to Josefin Starkhammar at Lund University for the great help with the design and construction of the new data acquisition system and as co-author. Anders Gudmarsson at Peab Asfalt is also gratefully acknowledged as a former colleague and for good cooperation during the work with Paper III. Discussions with, and ideas from, Peter Jonsson and Peter Ulriksen at Lund University are also greatly appreciated.

A great appreciation is also given to John Popovics at the University of Illinois at Urbana-Champaign and Suyun Ham at the University of Texas at Arlington, for valuable advice and discussions.

My gratitude also goes to the other Ph.D. students and the staff at the department of Civil and Architectural Engineering at KTH, and also to the members of the reference group, for fruitful discussions.

Last but not least, thanks to my family and friends for their support and encouragement during my years of studying.

Henrik Bjurström

Stockholm, January 2017

Appended papers

The presented thesis is based on four journal papers and one conference paper which are all appended in the end of this thesis. The papers present seismic testing methods on cement concrete slabs and asphalt concrete pavements. Papers I and V are focused on characterizing cement concrete slabs as a first step toward asphalt concrete while Papers III and IV are targeted on asphalt pavements. Paper II consists of a simulation, examining the findings of Paper I.

Paper I
Bjurström, H., Ryden, N., and Birgisson, B., 2016, Non-contact surface wave testing of pavements: comparing a rolling microphone array with accelerometer measurements, published in the special issue on *Advanced Sensing Technologies for NDE and SHM of Civil Infrastructures, Smart* Structures and Systems, 17 (1), 1-15. doi: 10.12989/sss.2016.17.1.001

Paper II
Bjurström, H. and Ryden, N., 2015, Effect of surface unevenness on in situ measurements and theoretical simulation in non-contact surface wave measurements using a rolling microphone array, presented at the 8th International Symposium on Non-Destructive Testing in Civil Engineering, 15-17 September, Berlin, Germany.

Awarded best poster at the conference poster competition.

Paper III
Bjurström, H., Gudmarsson, A., Ryden, N., and Starkhammar, J., 2016, Field and laboratory stress-wave measurements of asphalt concrete, published in *Construction and Building Materials*, 126, 508-516. doi: 10.1016/j.conbuildmat.2016.09.067

Paper IV
Bjurström, H. and Ryden, N., 2017, Non-contact rolling surface wave measurements on asphalt concrete, submitted for publication to *Road Materials and Pavement Design*.

Paper V
Bjurström, H. and Ryden, N., 2016, Detecting the thickness mode frequency in a concrete plate using backward wave propagation, published in the *Journal of the Acoustical Society of America*, 139 (2), 649-657. doi: 10.1121/1.4941250

Authors' contributions

Bjurström performed all tests and data analyses described in this thesis under the guidance of Ryden, except the laboratory tests and analyses described in Paper III that was performed by Gudmarsson.

Starkhammar and Bjurström designed, constructed and built the data acquisition system described in Papers III and IV after discussions with and advices from Ryden.

Bjurström wrote all text for all papers (except for Paper III where Section 2.2 "MEMS measuring system" was written by Starkhammar and Section 2.4 "Laboratory testing" was written by Gudmarsson). Bjurström acted as the corresponding author for all papers, and prepared and revised them for publication. Ryden assisted with comments during the preparation of all papers.

The work in Paper I was reviewed and commented by Birgisson.

Related publications

Bjurström, H. and Ryden, N., 2013, Air-coupled detection of the S1-ZGV Lamb mode in a concrete plate based on backward propagation, The 39th Annual Review of Progress in Quantitative Nondestructive Evaluation, Denver, Colorado, 15-20 July 2012, AIP Conference Proceedings, 1511, 1294-1300.

Bjurström, H. and Ryden, N., 2015, Effect of surface unevenness on non-contact surface wave measurements using a rolling microphone array, The 41st Annual Review of Progress in Quantitative Nondestructive Evaluation, Boise, Idaho, 20-25 July 2014, AIP Conference Proceedings, 1650, 128-135.

Awarded 3rd price in the annual conference student poster competition.

Bjurström, H., 2014, Air-coupled microphone measurements of guided waves in concrete plates, Licentiate Thesis, KTH Royal Institute of Technology, Stockholm, Sweden, ISBN 978-91-87353-51-2.

Bjurström, H., Gudmarsson, A., Ryden, N., and Starkhammar, J., 2016, Comparative seismic laboratory and non-contact field measurements of asphalt concrete, presented at NDE/NDT for Highway and Bridges: Structural Materials Technology, 29-31 August 2016, Portland, Oregon, published in NDE/NDT for Highway and Bridges: Structural Materials Technology 2016 Paper Summaries.

List of notations

E	Young's modulus
E^*	Complex modulus
E'	Storage modulus
G	Shear modulus
d	Plate thickness
ν	Poisson's ratio
ν^*	Complex Poisson's ratio
ρ	Density
V_P	Longitudinal wave velocity (P-wave velocity)
V_S	Shear wave velocity (S-wave velocity)
V_R	Rayleigh wave velocity
f_r	Impact Echo resonance frequency
β_{IE}	Impact Echo correction factor
θ	Refraction angle
A	Amplitude
f	Frequency
ω	Angular frequency
c	Phase velocity
c_T	Testing phase velocity
V_g	Group velocity
t	Time
x	Space
k	Wave number
k^*	Complex wave number
λ, μ	Lamé's constants (Section 2.1)
λ	Wavelength (except Section 2.1)
A_n	n^{th} higher antisymmetrical Lamb mode (n = 0, fundamental mode)
S_n	n^{th} higher symmetrical Lamb mode (n = 0, fundamental mode)
i	$\sqrt{-1}$
ε	Strain

List of abbreviations

AC	Alternating current
DC	Direct current
FE	Finite element
FFT	Fast Fourier transform
FWD	Falling weight deflectometer
GPR	Ground penetrating radar
IE	Impact Echo
MASW	Multichannel analysis of surface waves
MEMS	Micro-electro-mechanical sensor
MSOR	Multichannel simulation with one receiver
NDT	Nondestructive testing
QA/QC	Quality assurance/quality control
SASW	Spectral analysis of surface waves
ZGV	Zero group velocity

Contents

1 Introduction

In this thesis, seismic surface wave tests are performed on cement concrete and asphalt concrete in order to characterize elastic stiffness and layer thickness. The intention is to develop a nondestructive testing (NDT) method where seismic waves are transmitted, acquired, and evaluated using state of the art equipment. Non-contact measurement equipment, which enables surface tests to be performed while moving, is designed, built, and tested in this thesis. Data are collected almost continuously and the post-processing is made automatic to enable large scale quality assurance/quality control (QA/QC). The thesis stretches over multiple disciplines of research, such as equipment design, seismic wave theory, signal processing, and results interpretation.

1.1 Background

1.1.1 Asphalt concrete

Asphalt concrete is a composite material consisting of aggregates, bitumen, and air voids. Its mechanical behavior is complex due to its dependency of temperature, loading frequency, and strain level. The asphalt concrete is known to have a non-linear behavior at large strain. At larger strains than 50-100 με the asphalt concrete is considered to be viscoelastic-plastic, while it at lower strains is expected to have a linear viscoelastic behavior (Di Benedetto et al., 2001; Airey et al., 2003; Weldegiorgis and Tarefder, 2014). The seismic testing presented in this thesis exposes the asphalt concrete to strains in a range ~0.1 με and a linear viscoelastic material model can be adopted for all asphalt pavement tests in this thesis.

Design and QA/QC of pavements today are predominantly based on empirical values and prior experience. The finished multilayer asphalt concrete structure is evaluated by extracting numerous circular core samples and testing them in a laboratory environment. The air void content and the thickness of the pavement layers are regularly measured and compared to design values for verification (Trafikverket, 2011). The amount of cores taken for each built section is specified in the contracts but common amounts are ~4 cores/3000 m^2. An improved design is

required to become more generic and to be more focused on the mechanical properties instead of empirical values such as air void ratio. Today, there is an increased interest in mechanical based design and optimization of the life length and cost for pavement structures.

While materials like steel and cement concrete are rather straightforward to characterize for small strains using a constant Young's modulus, asphalt concrete is more complicated and requires a master curve to describe its behavior. The master curve characterizes the viscoelastic properties of asphalt concrete as a function of temperature and loading frequency. Using a master curve, moduli from the laboratory and the field may then be shifted and compared to each other even if the measurements are performed at different temperatures and/or frequencies. To construct the master curve, tests are performed on an asphalt concrete specimen at specified temperatures inside a temperature chamber to determine the complex moduli. By calculating shift factors, these moduli may then be shifted to describe the material properties over wider temperature and frequency ranges.

1.1.2 Field NDT

There are some different NDT methods available to characterize the asphalt concrete properties in pavements. Ground penetrating radar (GPR), nuclear density gauge, and different deflection basin methods are all methods where measurements are obtained in order to evaluate different parameters of the asphalt concrete layers. GPR is applied by transmitting and receiving short pulses of electromagnetic energy and can be utilized to estimate layer thicknesses and locating subsurface objects (Blindow et al., 2007; Saarenketo and Scullion, 2000), detect moisture (Al-Qadi et al., 1991), estimate air void content (Saarenketo, 1997), and determine density (Al-Qadi et al., 2010). The nuclear density gauge is a device which emits gamma radiation that is being reflected back into the device. Using the concentration of reflected gamma rays, the density can be estimated. Due to the hazards involved in handling radioactive material using the nuclear density gauge, a non-nuclear electrical gauge was developed that utilizes impedance measurements at specified frequencies of alternating current (AC) (Schmitt et al., 2006).

There are some different deflection basin methods available but they all rely on measuring the pavement surface deflection due to a known load which enables characterization of the dynamic modulus. Depending

on the loading conditions and how the response is measured, these methods are called static loading, steady state loading, or transient loading. The most common method is the falling weight deflectometer (FWD), where a transient load is applied and the deflection response is measured at several specified locations along a radial line (Ioannides et al., 1989). Such a deflection basin represents an overall stiffness of the complete multilayered pavement structure and a backcalculation routine is then needed to estimate the mechanical properties for the individual layers. However, backcalculating deflection data always entails uncertainties and the overall stiffness has also been shown to be more sensitive to the thick unbound layers and less sensitive to the thinner, stiffer asphalt concrete layers (Aouad et al., 1993).

Ideally, any field test method should be able to be linked to laboratory measurements where the asphalt concrete mix is usually developed. Laboratory tests can be performed in a controlled environment where the loading frequency and especially the temperature can be governed. Repeated testing over wide ranges of frequencies and temperatures can lead to viscoelastic material characterization.

1.1.3 Laboratory NDT

Conventional laboratory tests to characterize the viscoelastic properties of asphalt concrete can be performed by exposing a core specimen with specified dimensions to cyclic loading. A stepwise frequency sweep over 0.01-25 Hz is applied at different temperatures to measure the response (American Association of State Highway and Transportation Officials (AASHTO), 2007). Figure 1(a) shows the Simple Performance Tester in which the tests are performed. Cyclic loading tests require meticulous setup and are time consuming, require skilled operators, and the equipment is very expensive. Despite these disadvantages, the cyclic loading test is the most common method applied to characterize the viscoelastic properties of asphalt concrete today.

Seismic laboratory testing has recently been developed for asphalt concrete specimens. A photo of the equipment needed to perform the testing is shown in Figure 1(b). The frequency response from a transient

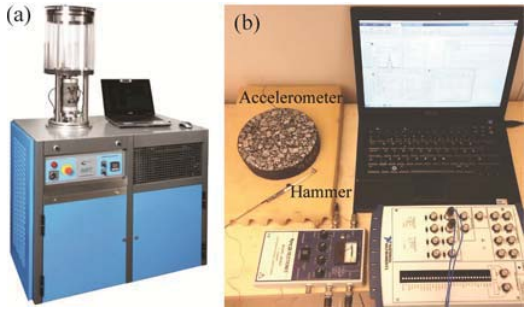

Figure 1: (a) Photos of the Simple Performance Tester (Labs4u, 2017) and (b) seismic laboratory testing equipment (Gudmarsson, 2014).

impact on an asphalt concrete specimen is measured. By fitting a finite element (FE) model to the measurement results, viscoelastic parameters, such as the complex modulus E^* and the complex Poisson's ratio ν^*, can be extracted from the model. The assumption that asphalt concrete is a thermo-rheologically simple material (Nguyen et al., 2009) allows for shifting the measured complex moduli into a unique master curve, representing the moduli measured in a limited frequency range over a wider frequency range at a chosen reference temperature. Shift factors are calculated using the temperature at which the specific modulus was tested, the reference temperature, and two material constants. The shifting is then performed by multiplying the shift factor and the frequency to obtain reduced frequency (Gudmarsson et al., 2012).

The seismic laboratory testing has several advantages compared to the conventional laboratory testing. It is easy to perform and does not require extensive training, neither is the equipment very expensive. It is also performed in the same frequency range as the seismic field testing. A master curve demonstrating how the complex modulus varies with frequency is plotted in Figure 2, where the approximate frequency ranges where cyclic loading tests and seismic tests are performed, are marked.

Both seismic tests (laboratory and field) are performed at low strain ($\sim 10^{-7}$) and can therefore be directly linked.

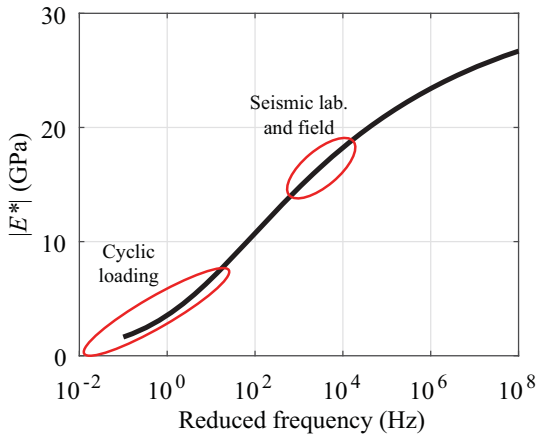

Figure 2: Master curve demonstrating how the complex modulus *E varies with frequency. The frequency ranges at which the cyclic loading tests and seismic tests (laboratory and field) are performed, are marked.**

1.1.4 Pavement testing today

Quality control of pavements is today mainly based on examining core specimens, a destructive test method that relies on sparse evaluated values. Numerous circular cores are extracted from newly built roads in Sweden and analyzed in laboratory environment. The cores are examined to determine air void content and thickness of the asphalt concrete layer. The air void content is compared to table values specified by the Swedish Transport Administration (Trafikverket, 2011) to verify that the desired packing quality has been achieved. Mechanical properties like the material stiffness are neither examined in the current QA/QC process, nor accounted for, which makes pavement design today empirical and not based on performance specifications. Furthermore, core samples only provide information about the specific positions where the cores have been taken and no continuous information along the pavement is evaluated. There is a need for a more analytical QA/QC process that is based on the actual material stiffness to increase the knowledge level for the material.

Stiffness and thickness of pavement layers are the two most important parameters that determine the bearing capacity and lifetime of

pavements (Said, 1995). Cracks, that occur due to large strains, and rutting (plastic or permanent deformation) are the two main failure modes. Today there is an increasing interest for pavement design based on mechanical properties; hence, there is an increasing need for reliable measurements and evaluation methods for properties such as the stiffness and layer thickness.

One interesting test method that is investigated in this thesis is seismic wave testing. Seismic waves are stress waves, caused by a disturbance somewhere in the material, propagating with small strains in solid materials. The waves carry information about material stiffness which can be, if treated correctly, used to characterize the material, e.g. seismic waves travel faster in stiffer materials. Surface waves are seismic waves propagating along the free surface or an interface in a half space or a layered system. These waves can be acquired at the surface and utilize material characterization and damage detection.

The work presented in this thesis is based on such surface wave testing performed on cement concrete slabs (Papers I and V) and the top asphalt concrete layer of pavements (Papers III and IV).

1.2 Objectives

The main objective with the presented thesis is to develop NDT for pavements using seismic wave propagation, based on non-contact surface wave measurements for characterization of the stiff top layer of the pavement. The intention is to implement and demonstrate fast data acquisition and robust data evaluation routines to facilitate future large scale testing. Properties such as stiffness and thickness are key parameters for the structural capacity and need to be determined in a rapid and nondestructive manner. Furthermore is the aim to verify that the dynamic high frequency modulus obtained using seismic field testing, is equivalent to that of seismic laboratory testing.

1.3 Methods

A new data acquisition system for field measurements is designed and built. Multiple field studies are performed using both an older and this new system, where data are acquired from cement concrete slabs in Papers I and V and asphalt concrete pavements in Papers III and IV. Numerical modeling is performed in Paper II to introduce measurement

errors and study their effects on the calculated results. Core specimens are extracted in Paper III to perform laboratory tests for comparison with field testing.

1.4 Limitations

The number of test sites in this project is limited. The results presented in this work should thus not be seen as fully validated test methods but rather demonstrations of future possibilities.

In Paper III and IV, surface wave measurements are obtained from asphalt concrete pavements. The temperatures, at which the tests are all performed, are in a limited range. However, this temperature range is rather high; tests at lower temperatures are expected to provide equally good or better results due to less seismic attenuation. The examination of asphalt concrete pavements is also limited to the stiff asphalt concrete top layer. No inversion of the underlying unbound layers is performed.

All field tests performed in this study are aimed at determining the wave propagation velocity and evaluating the dynamic modulus, linear elastic theory is thus applied. Viscous properties may also be evaluated by studying the wave attenuation; however, this requires well calibrated instruments and is omitted from this project.

All tested structures are assumed to be isotropic and homogeneous in this project. It cannot be excluded that anisotropy could influence the measurements to some degree. However, the surface waves have a particle motion in both the vertical and horizontal (propagation) directions and the calculated moduli can thus be assumed to represent an average value for the examined material.

Both cement concrete and asphalt concrete are composite materials and are not truly homogeneous. When performing seismic testing at high frequencies, large aggregates cause refraction and wave scattering. A method to neutralize the problem of scattered waves was introduced by Chekroun et al. (2009). However, in this project the studied wavelengths exceed the aggregate size which significantly decreases the refraction and scattering of waves (Bernard et al., 2014).

2 Seismic waves

Elaboration on surface wave theory, on which the measurements presented in this thesis are based, is presented in this chapter. Surface waves and Lamb waves are the main types of waves utilized in this thesis and will be given the main focus.

2.1 Body waves

In an infinite material space, two different types of waves can propagate: the compressional wave and the shear wave. Each wave type is characterized by a material specific velocity. The compressional wave is defined by a particle motion in the wave propagation direction and it has always the highest wave speed. It is therefore also referred to as the primary wave or the P-wave. The shear wave has a particle motion transverse to the wave propagation direction. It has a lower wave speed compared to the primary wave and is also referred to as the secondary wave or the S-wave. Primary and secondary waves are together called body waves or bulk waves. The propagation of P- and S-waves is depicted in Figure 3.

The P-wave velocity V_P and the S-wave velocity V_S are dependent on the mechanical properties of the material and they relate to the Young's modulus E according to Equations 1 and 2, respectively,

$$V_P = \sqrt{\frac{\lambda + 2\mu}{\rho}} = \sqrt{\frac{E(1-\nu)}{\rho(1+\nu)(1-2\nu)}}, \tag{1}$$

$$V_S = \sqrt{\frac{\mu}{\rho}} = \sqrt{\frac{E}{2\rho(1+\nu)}}, \tag{2}$$

where λ and μ are Lamé's constants, ρ is the material density, and ν is the Poisson's ratio. The ratio between V_S and V_P can be expressed using only the variable ν as in Equation 3.

$$\frac{V_S}{V_P} = \sqrt{\frac{1-2\nu}{2(1-\nu)}} \tag{3}$$

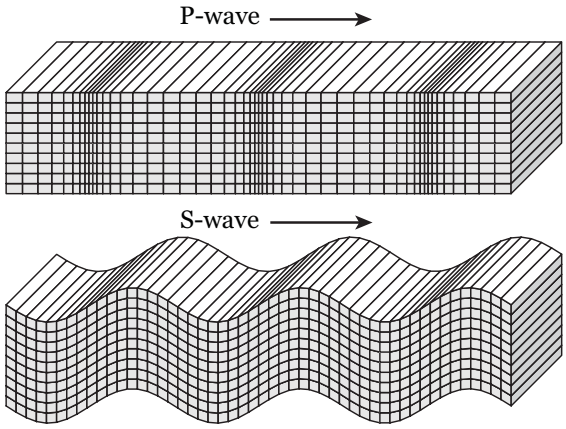

Figure 3: Longitudinal wave (P-wave) and transversal wave (S-wave) patterns illustrated for a horizontal wave propagation direction according to the arrows. (Figure from Shearer (1999))

2.2 Guided waves

2.2.1 Surface waves

Only body waves can exist in an infinite material space. However, when the material does not extend to infinity but one or more surfaces are present, other types of waves are generated. These waves are called surface waves since they are confined close to the surface. The most important type of surface wave is the Rayleigh wave, which at the surface has a retrograde particle motion in relation to its propagation direction. The shape of the Rayleigh wave is illustrated in Figure 4. The wave motion is elliptical but the major displacement takes place in the vertical direction. The particle motion decays exponentially and can be normalized with respect to wavelength λ according to Figure 5, where u and w are the displacement in the vertical and horizontal (propagation direction) directions, respectively. It can be seen in Figure 5 that at a rather shallow depth (~0.16λ), the horizontal particle motion component goes from positive to negative, meaning that the particle motion goes from retrograde to prograde.

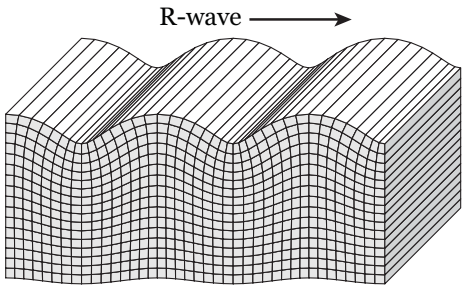

Figure 4: The Rayleigh wave (R-wave) has an elliptical particle motion; the motion is counterclockwise at the surface for a wave propagation direction according to the arrow. Thus, the particles move both in the longitudinal and the transversal directions. (Figure from Shearer (1999))

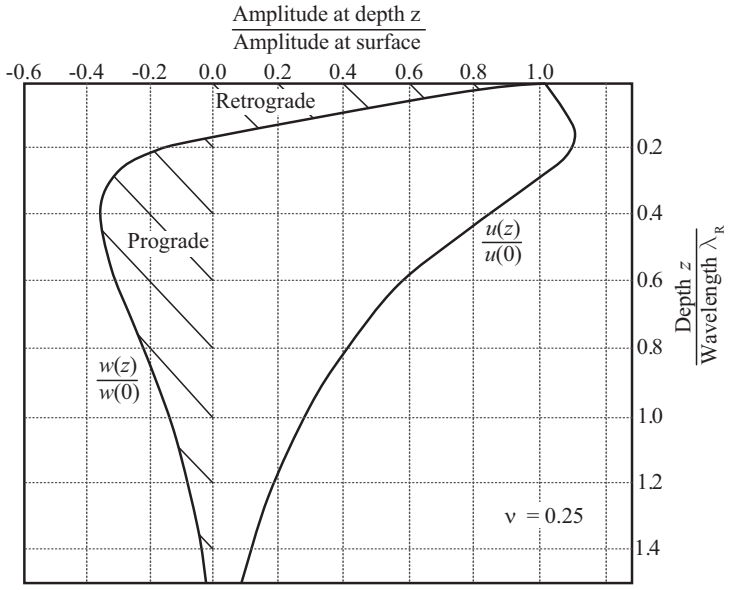

Figure 5: Vertical (u) and horizontal (w) particle motions of the Rayleigh wave plotted for depth down to 1.5 wavelengths. Poisson's ratio is set to 0.25. (Figure after Richart et al. (1970))

The Rayleigh wave contains approximately two thirds of the energy induced from an impact source on the surface and will show larger amplitude on the surface compared to the body waves. In a half-space, the Rayleigh wave propagates radially outward from the impact source along a cylindrical wave path while the body waves have a hemispherical wave path according to Figure 6. All waves will hence be spread over an increasing material volume when propagating, which causes the energy to dissipate. This is called geometrical damping. Body wave amplitude decreases with the radial distance r from the impact source in proportion to the ratio $1/r$ inside the material and as $1/r^2$ along the surface. The Rayleigh wave, which is only propagating along the half-space surface, decreases in amplitude with only $1/\sqrt{r}$. This facilitates the measuring of surface waves instead of body waves at a distance away from the impact source. The wave propagation velocities and their relative amplitudes are depicted in Figure 6 for a material with $\nu = 0.25$.

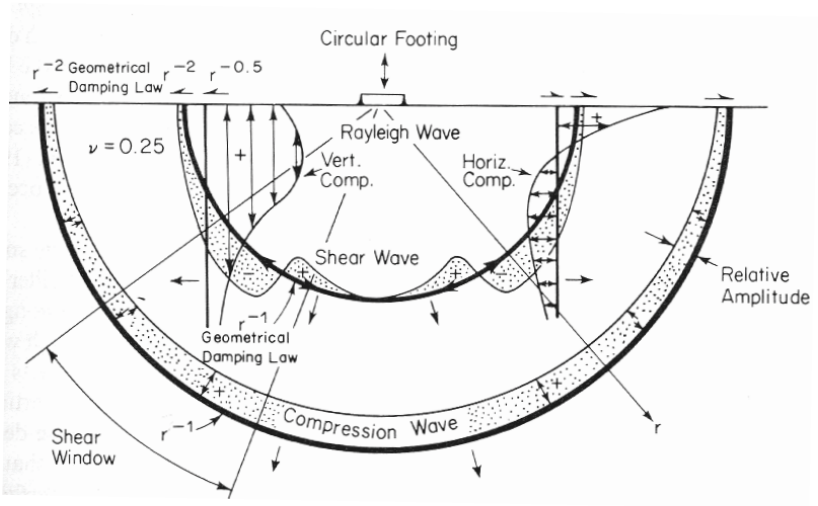

Figure 6: Relative wave propagation velocity distribution for $\nu = 0.25$. (Figure from Richart et al. (1970))

The propagation velocity of the pure Rayleigh wave (V_R) is slightly lower than V_S and the ratio between the two is dependent on the ratio

V_S/V_P, i.e. on Poisson's ratio. Lord Rayleigh's dispersion relation (Rayleigh, 1885) in Equation 4 describes the relation between velocities.

$$-4\frac{V_S^2}{V_R^2}\sqrt{\frac{V_S^2}{V_R^2}-\frac{V_S^2}{V_P^2}}\sqrt{\frac{V_S^2}{V_R^2}-1}+\left(1-2\frac{V_S^2}{V_R^2}\right)^2=0 \qquad (4)$$

Different simplifications of Equation 4, giving similar results, have been presented by several authors (Bergmann and Hatfield, 1938; Gibson and Popovics, 2005); however, one commonly used was presented by Nazarian et al. (1999) and is given in Equation 5.

$$V_R=\frac{V_S}{1.13-0.16\nu} \qquad (5)$$

Seismic wave velocities are related to the dynamic moduli of the material so that higher wave velocities come with a stiffer material (higher moduli). The dynamic shear modulus G relates directly to the shear wave velocity through Equation 6:

$$G=\rho V_S^2, \qquad (6)$$

where ρ is material density. Using G, the dynamic Young's modulus can be calculated with Equation 7 once the Poisson's ratio is known or can be assumed.

$$E=2G(1+\nu) \qquad (7)$$

2.2.2 Lamb waves

Propagating stress waves that are constrained by two parallel surfaces (plate) are called Lamb waves (Lamb, 1917). Plates are also called waveguides and the propagating waves are called guided waves since they are guided by the material boundaries. The behavior of Lamb waves and surface waves can be fully characterized by superposition of interacting P- and S-waves and the boundary conditions of the structure. Pure Lamb waves are only valid for free plates, i.e. an isotropic homogeneous plate with infinite lateral dimensions and with vacuum on both sides of the interfaces. However, Lamb wave theory can be approximately used

without any large errors for plate structures where adjacent layers have much lower stiffness (Ryden et al., 2003). Lamb waves cause the plate to deform according to one out of two wave mode groups: symmetrical (S) or antisymmetrical (A) Lamb modes, see Figure 7. The symmetrical and antisymmetrical labels refer to the average particle displacement around the horizontal midplane of the plate.

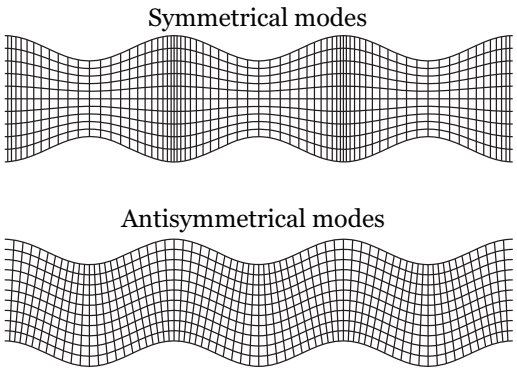

Figure 7: Lamb modes are divided into symmetrical and antisymmetrical mode groups which refer to the average particle motion around the horizontal midplane of the plate.

There are an infinite number of individual symmetrical and antisymmetrical Lamb modes where higher order modes correspond to more nodal points in the thickness direction and shorter wavelengths. Wave propagation is only possible for certain combinations of frequencies (f) and phase velocities (c), given by the dispersion equation (Lamb, 1917) in Equation 8:

$$\frac{\tan\left(\beta\frac{d}{2}\right)}{\tan\left(\alpha\frac{d}{2}\right)}+\left(\frac{4\alpha\beta k^2}{\left(k^2-\beta^2\right)^2}\right)^{\pm 1}=0\,, \qquad (8)$$

where

$$\alpha^2 = \frac{\omega^2}{V_P^2} - k^2 , \quad (9)$$

$$\beta^2 = \frac{\omega^2}{V_S^2} - k^2 , \quad (10)$$

d being the plate thickness, ω being the angular frequency ($\omega = 2\pi f$), and k being the in-plane wave number ($k = \omega/c$). The ±1 exponent on the second term in Equation 8 accounts for symmetrical (+1) and antisymmetrical (-1) modes of vibration. Three structural parameters need to be set to derive the dispersion curves, e.g. V_S, d, and ν. The dispersion equation (Equation 8) is a transcendental equation and it is not straightforward to solve. Instead, a root searching algorithm must be applied where a set of wave number roots may be found for every frequency examined; a larger set of roots may be found at higher frequencies compared to lower frequencies. Wave numbers are generally complex but if only propagating modes are considered, the imaginary parts can be neglected (Achenbach, 1998). In Figure 8, the dispersion curves of the three first A- and S-modes are displayed. The x- and y-axes are normalized with respect to plate thickness d and shear wave velocity V_S, respectively. This way, the dispersion curves become valid for all values of V_S and d, and only need to be derived once for every new value of Poisson's ratio.

The dispersion curves are employed in the journal papers attached to this thesis. By fitting one or more dispersion curves to measurement data, characteristics of the tested plate structure, such as shear wave velocity, plate thickness and Poisson's ratio, can be determined by backcalculation.

To determine the wave propagation velocities, and subsequently the real part of the dynamic moduli, it is sufficient to use the real parts of the dispersion curves. However, to explain the theory behind waves with counter-directed phase velocity and group velocity, utilized in Paper V, to identify the minimum frequency of the S_1 mode, complex dispersion curves need to be derived. This implies using complex wave numbers k^* that contain a real part k_r and an imaginary part k_i according to Equation 11.

$$k^* = k_r + i \cdot k_i \quad (11)$$

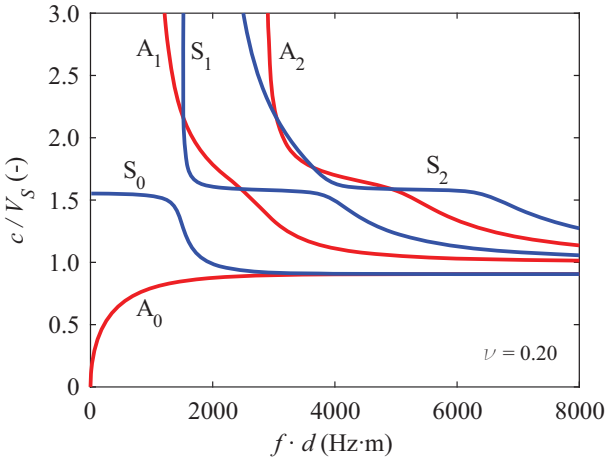

Figure 8: Real valued dispersion curves normalized with respect to plate thickness and shear wave velocity. ν = 0.20.

The real and imaginary parts of the complex wave numbers then need to be varied independently in a similar manner as for the calculation of real valued dispersion curves, to find the roots to Equation 8 at each frequency.

The group velocity V_g is defined as the velocity at which the energy propagates and is given by the slope of the dispersion curve in angular frequency and wave number domain according to Equation 12.

$$V_g = \frac{d\omega}{dk} \tag{12}$$

By studying the imaginary parts of the dispersion curves alongside with their real parts, some Lamb modes can be demonstrated to have interesting properties. The S_1 mode is especially interesting to study for the new alternative thickness determination method presented in Paper V. The group velocity can be shown to vanish for a certain non-zero wave number; this point is later referred to as the $S_{1\text{-ZGV}}$ point, ZGV representing “zero group velocity”. Tolstoy and Usdin (1957) described this phenomenon as that the energy would be trapped and not propagate, and associated this state with some kind of resonance or ringing effect.

Mindlin (1960) further explained that what appears to be the S_1 mode for lower wave numbers than this point on the dispersion curve, in fact is a part of the S_2 mode called S_{2b}, where the index b represents a "backward wave". The term backward wave refers to a propagating wave with phase velocity and group velocity with opposite signs, i.e. waves propagating from an impact source toward a receiving sensor but with a phase velocity directed backwards.

Complex dispersion curves for a free plate with $V_S = 2360$ m/s, $d = 0.3$ m, and $\nu = 0.18$, representing the cement concrete slab evaluated in Paper V, are calculated and plotted in Figure 9. The dispersion curves correspond to the first two higher symmetrical modes in the positive (S_1 and S_2) and negative (S_{-1} and S_{-2}) x-directions. The curves are plotted in 3D in Figure 9(c) with their projections on the planes $k_r = 0$, $k_i = 0$, and $f = 0$ in Figure 9(a), (b), and (d), respectively.

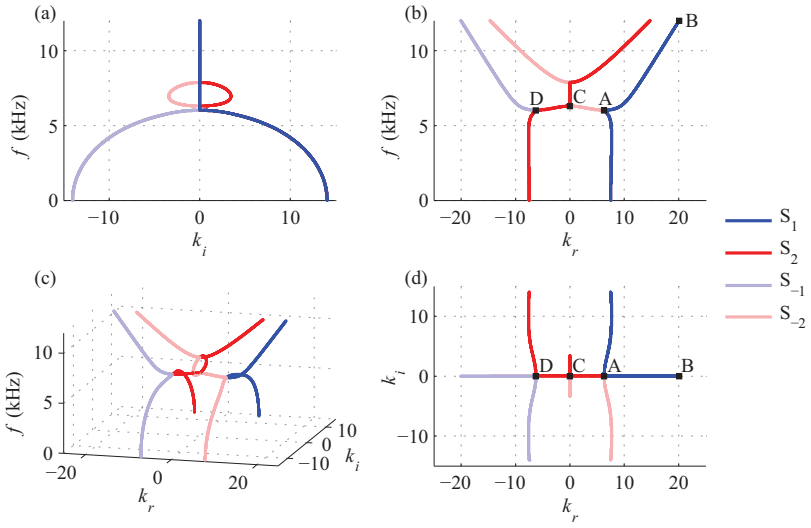

Figure 9: Complex dispersion curves calculated for a cement concrete plate with $V_S = 2360$ m/s, $d = 0.3$ m, and $\nu = 0.18$. The curves are plotted (c) in 3D with their projections on the planes (a) $k_r = 0$, (b) $k_i = 0$, and (d) $f = 0$. (Figure after Mindlin (1960) and Simonetti and Lowe (2005))

To gain further understanding of complex dispersion curves, it is important to first define a consistent coordinate system. A free plate is considered in 2D in Figure 10 where a transient impact is applied at $x = 0$. Lamb waves will then propagate in both directions, both from the source toward the microphone (x>0), and from the source away from the microphone (x<0). This implicates the use of negative mode indices, Lamb waves with a negative mode index are propagating in the negative direction from the impact source (negative group velocity) according to the definition of positive and negative directions in Figure 10. In a homogeneous plate with infinite lateral dimension, the energy propagation (group velocity) can never change direction. It is therefore only Lamb modes with a positive index that can be measured by the microphone in Figure 10. However, the phase velocity is given by the wave number; positive wave numbers come with positive phase velocities and vice versa. Mindlin (1960) explained that since the wave number is only given to the power of two in the dispersion equation (Equation 8), the positive and negative solutions must be equally correct and the complex dispersion curves are thus mirrored around the planes $k_r = 0$ and $k_i = 0$ (see Figure 9).

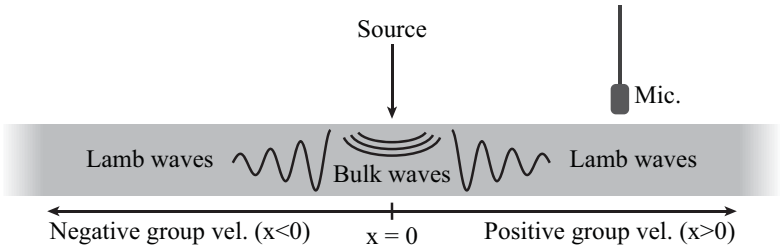

Figure 10: Schematic of a free plate with infinite lateral dimensions. A consistent coordinate system is defined to elaborate on the phase velocity and group velocity in the positive and negative directions.

The main interest in Figure 9 is right between the points A and D. Solving the dispersion equation for real valued wave numbers exclusively, these two points will appear to be the same and that the curve BAC in Figure 9 would all be the S_1 mode. However, in Figure 9(b) it is established that the S_1 mode only exists for real wave numbers larger than point A. What appears to be the S_1 mode exclusively at a frequency

infinitesimally higher than the $S_{1\text{-}ZGV}$ point (point A) at the microphone in Figure 9 is in fact the S_1 mode between B and A, and the S_2 mode between D and C in Figure 8(b). It is thus a matter of two waves (S_1 and S_2) with the same absolute phase speed but with opposite signs, causing the resonance. The S_2 mode with negative wave numbers (negative phase velocities) is concluded to be detectable in a narrow frequency range (DC in Figure 9) close to the minimum frequency of the real valued S_1 and S_2 modes.

3 Background of seismic testing

The primary objective of the work conducted for this thesis is to achieve rolling surface wave measurements that are fast and reliable. This is important to enable large scale NDT of pavements in the future. Previously, geophones and accelerometers have been widely used to acquire surface wave data at test sites such as soil surfaces, cement concrete structures and asphalt pavements. However, large scale testing has been hampered by the need for full contact between the receiving sensor and the material surface. Attaching sensors to the surface is not only time consuming, it can also be difficult to achieve on rough surfaces or to repeat when multiple measurements need to be compared.

3.1 Non-contact testing

Different sorts of non-contact receivers have been employed for various seismic test methods for decades. Pioneering work was presented by Luukkala et al. (1971), demonstrating fully non-contact wave transmission through thin paper sheets. Single sided generation and detection of Lamb waves in the ultrasonic range were presented by Castaings and Cawley (1996) on steel plates. Ability to transmit and receive signals from the same side is required in many cases due to the limited access of the tested structure (e.g. pavements). Zhu and Popovics (2002) demonstrated how an air-coupled directional microphone can be employed to detect and acquire the out-of-plane displacement in the audio frequency range on cement concrete slabs. Later on, they presented a study where the same sort of directional microphone collected leaky surface waves for detection and imaging of surface-opening cracks on a cement concrete slab (Zhu and Popovics, 2005). Material characterization of cement concrete, using automated and fully non-contact ultrasonic systems, were developed and presented by Piwakowski and Safinowski (2009) and Abraham et al. (2012). Various setups have been employed by many authors and for different purposes, such as evaluation of bridge deck delamination (Kee at al., 2011), determining depth of surface-breaking cracks (Kee and Zhu, 2010), and characterizing the amount of microcracks (Ham et al., 2017) in concrete. A rolling

multichannel microphone array was designed by Ryden et al. (2008), enabling rapid surface wave tests performed on-the-fly.

The rolling microphone array is also the starting point for the work presented in this thesis. The overall goal with this work is to enable rolling non-contact surface wave measurements using air-coupled microphones as receiving sensors in order to assess dynamic moduli and thickness of pavements. Continuous measurements can possibly enable future QA/QC of pavements based on mechanical properties. This would not only provide more covering results, it would also be expected to substantially lower the cost and the time needed for QA/QC.

3.2 Air-coupled microphones as receivers

Surface wave data acquisition can be performed using different kinds of sensors. Accelerometers measure the surface acceleration over time at the accelerometer locations. Air-coupled microphones do not measure acceleration but air pressure that is being proportional to air velocity at the acoustic port of the microphones. Acceleration or velocity is in this case irrelevant since it is only the relative phase difference between the multiple signals that is used in the evaluation of phase velocity.

A supersonic surface wave propagating along a free surface of a solid will leak energy into the adjacent air, this leaky energy will refract at an angle θ according to Snell's law:

$$\theta = \arcsin\left(\frac{c_1}{c_2}\right), \tag{13}$$

where c_1 and c_2 are the phase velocities of the higher (plate) and lower (air) velocity materials, respectively. Therefore, there is an inherent limitation that a propagating surface wave can only refract (leak) into the lower velocity material.

3.3 Data evaluation

Today, there is a wide variety of available NDT methods using seismic waves. Characterization of cement concrete pavements was demonstrated using steady state measurements by van der Poel (1951) and Jones (1955). The response from a vibrator source was measured at multiple offsets

using a geophone. Using frequency and wavelength data determined by identification of the amplitude maxima as a function of distance from the source, dispersion curves could subsequently be derived. Similar results were presented by Heukelom and Foster (1960) where measured dispersive phase velocities were interpreted to characterize the multilayered structure. Phase velocity shifts at specific wavelengths were interpreted as subsurface layer interfaces when the affected depth was considered to be half the Rayleigh wavelength, see Figure 11.

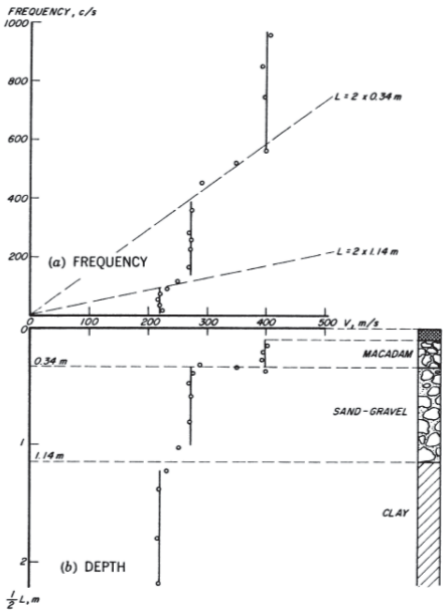

Figure 11: Evaluation of surface wave data is utilized to assess the properties of the multilayered structure. Phase velocity shifts at specific wavelengths were interpreted as subsurface layer interfaces (Heukelom and Foster, 1960).

The spectral analysis of surface waves (SASW) method was first introduced by Heisey et al. (1982) as a development of the steady state measurements. The analysis method is based on two simultaneous geophone measurements, radially separated from a transient impact, and determination of a single continuous dispersion curve by unwrapping the

phase spectrum. Compared to the steady state measurements, the SASW method is fast due to the ability to excite a wide range of frequencies from a single impact. Surface wave measurements utilizing the SASW method compared to crosshole measurements (Hoar and Stokoe, 1978) demonstrated that elastic moduli could be estimated from measured Rayleigh wave velocities for a multilayered flexible pavement system. Several studies have been presented since then, providing an improved SASW method able to assess moduli and thicknesses of both flexible and rigid multilayered pavement systems (Nazarian et al., 1983; Roesset et al., 1990; Rix et al., 1991). However, several authors have presented problems and limitations regarding the SASW method (Hiltunen and Woods, 1990; Al-Hunaidi, 1992; Tokimatsu et al., 1992), most of them related to difficulties of phase unwrapping and the ambiguity caused by present higher order modes which are difficult to detect due to the limited number of transducers.

In Papers I, III, and IV in this thesis, multichannel data records are collected using multiple receiving sensors acquiring data simultaneously from a single impact. In Paper V, an equivalent multichannel data record is created using a single receiving sensor and multiple impacts. In the latter case, the data acquisition is triggered using the impact source to synchronize the offsets in the data record (Ryden et al., 2004). Park et al. (1998, 1999) introduced the multichannel analysis of surface waves (MASW) that allows a multichannel data record to be transformed into multimodal dispersion curves. MASW is basically a 2D Fourier transform, where multichannel data records in time-space can be transformed into multimodal dispersion curves in frequency-phase velocity domain. If the multichannel data record in time-space domain is denoted $u(x,t)$, the same data record may be presented in space-frequency domain $U(x,\omega)$ using a fast Fourier transform (FFT) in Equation 14.

$$U(x,\omega) = \int u(x,t) e^{i\omega t} dt \,, \tag{14}$$

$U(x,\omega)$ may be divided into two factors:

$$U(x,\omega) = A(x,\omega) P(x,\omega) \,, \tag{15}$$

where $A(x,\omega)$ and $P(x,\omega)$ contain the amplitude and phase information, respectively. $A(x,\omega)$ is the term reflecting the attenuation and $P(x,\omega)$

contains all information about phase velocity *c* of each frequency *f* (angular frequency $\omega = 2\pi f$) according to Equation 16.

$$P(x,\omega) = e^{-i\Phi(x,\omega)} \tag{16}$$

where

$$\Phi(x,\omega) = \omega\frac{x}{c} \tag{17}$$

If an arbitrary single frequency is considered, the data record will be represented by multiple sinusoid curves at different offset *x* from the impact source, with the same frequency but with different phase and different amplitude. Since $A(x,\omega)$ is governed by the amplitude and attenuation, and contains no information about phase velocity, $U(x,\omega)$ may be normalized according to Equation 18 without any loss of significant information for phase velocity determination.

$$U_{norm}(x,\omega) = \frac{A(x,\omega)}{|A(x,\omega)|}\cdot P(x,\omega) = P(x,\omega) \tag{18}$$

Finally, the measurement data in $U_{norm}(x,\omega)$ may be transformed into frequency-phase velocity domain using Equation 19;

$$S_{norm}(\omega,c) = \int U_{norm}(x,\omega)\cdot e^{-i\frac{\omega}{c_T}x}\,dx\,, \tag{19}$$

which basically is a summation of signal amplitudes for time shifts between signals corresponding to the testing phase velocity (c_T). Similar methods to capture the dispersion characteristics of propagating waves also appear with different names, such as the slant stack transform (Ambrozinski et al., 2014).

Graphically this process can be explained by studying a single frequency. A synthetic multichannel data record with *n* signals, corresponding to a surface wave with arbitrary frequency and phase velocity of 22 kHz and 2000 m/s, respectively, is plotted in Figure 12(a). The continuous displacement in space (*x*) and time (*t*) is then given by Equation 20:

$$u(x,t) = Ae^{kx-\omega t}, \qquad (20)$$

where the amplitude *A* in this case can be set to 1.0. All signals will have the same phase in a slope corresponding to an arbitrary phase velocity, here *c* = 2000 m/s. At almost all other slopes (phase velocities), the phase will be different for the multiple signals. By summing all signal amplitudes, a best fit optimally corresponding to the true phase velocity, can be located. In Figure 12(b), this summation is depicted for different numbers of signals. In Figure 12(c), a wide range of included signals *n* for the synthetic data record is tested and given on the x-axis. The summed and normalized amplitude is given in black (high) and white (low) and can be seen to converge to the theoretical phase velocity.

From Figure 12, it can be concluded that a higher number of signals will provide more robust results, or higher resolution. This is one of the main reasons for utilizing a high number of signals in surface wave testing.

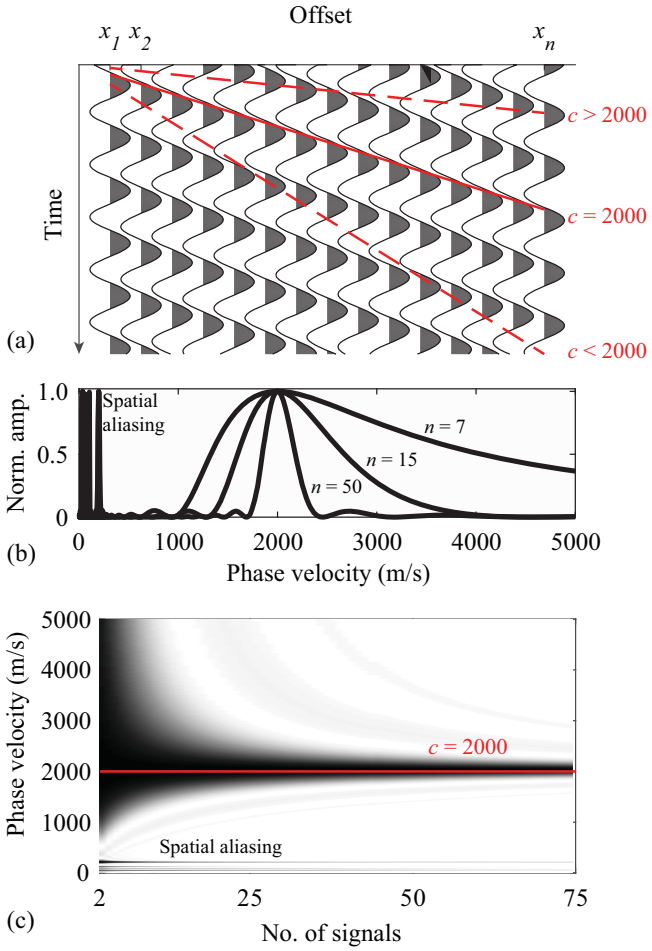

Figure 12: (a) A synthetic multichannel data record corresponding to a surface wave with a frequency and phase velocity of 22 kHz and 2000 m/s, respectively. (b) The amplitudes from the different number of signals used are summed and normalized and (c) the same summation but for all numbers of receivers between 2 and 75.

3.4 Impact Echo

Using surface wave testing, seismic wave velocities and subsequently the stiffness moduli may be determined. However, with non-contact receivers

it is generally difficult to determine layer thicknesses using surface wave data without applying a complicated and ambiguous inversion process.

However, using an accelerometer receiver it is often rather straightforward to determine the thickness. Impact Echo (IE) is a NDT method, developed by Sansalone and Carino (1986), for thickness determination and flaw detection in cement concrete. A mechanical impact is applied on the surface of the examined material and the response is measured by a transducer in the vicinity of the impact point. The response is transformed into frequency domain using a Fourier transform. Multiple reflections of stress waves between the two external surfaces, or the impact surface and an internal flaw, cause a resonance at a frequency proportional to the thickness of the delaminated portion or the entire slab. Using this resonance frequency f_r, the thickness d (or thickness above any flaw) can be calculated using Equation 21:

$$f_r = \frac{\beta_{IE} \cdot V_P}{2d} \tag{21}$$

once the P-wave velocity is known or can be estimated. β_{IE} is a correction factor that is dependent on ν (Gibson and Popovics, 2005).

However, due to low signal-to-noise ratio, the IE method has been shown to be difficult to apply using air-coupled microphones as receivers. To overcome this problem, different solutions have been presented. Zhu and Popovics (2007) presented a study where an insulation was designed and surrounded an air-coupled microphone for IE testing. Dai et al. (2011) constructed a parabolic reflector, focusing the refracted energy to enhance the signal-to-noise ratio. An array based IE sensor employing micro-electro-mechanical sensor (MEMS) microphones was designed by Groschup and Grosse (2015). They demonstrated how multiple sensors, mounted in a sophisticated pattern, could improve the collective IE signals significantly.

4 Data acquisition

Different data acquisition systems, and also different methods to acquire data, are used in the work on which this thesis is based. In Chapter 4, these systems, constructed using different equipment and methods, will be explained.

4.1 Data acquisition methods

Two different but equivalent data acquisition methods are used in the work presented in this thesis: true multichannel measurements and multichannel simulation with one receiver (MSOR) (Ryden et al., 2001).

4.1.1 True multichannel measurements

True multichannel measurements are applied in most studies where air-coupled microphones are used in this thesis. Simultaneous data collection on multiple receivers enables a multichannel data record to be created from a single impact. This is depicted in the schematic in Figure 13. All equipment needed to perform the non-contact measurements in Paper I is illustrated in Figure 13 and further explained in Section 4.2.1.

Since all receivers collect data simultaneously, the data collection may be triggered on one of the receivers. This is opposed to the MSOR method where the absolute time from impact to receiver needs to be recorded for each signal.

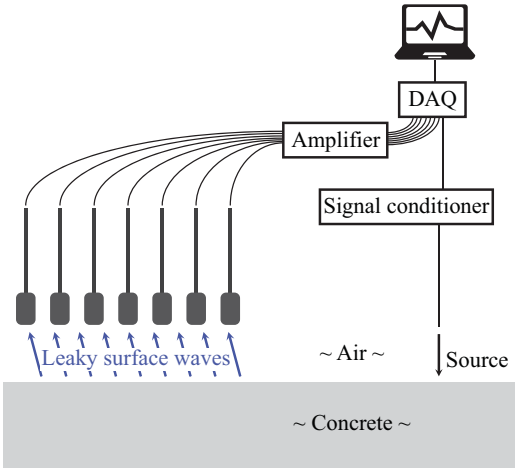

Figure 13: Schematic of the true multichannel measurement setup used in Paper I. The data acquisition device is denoted DAQ.

4.1.2 Multichannel simulation with one receiver

The MSOR approach is a method to simulate the true multichannel measurements explored in Section 4.1.1. Instead of simultaneously collecting data on multiple receivers from a single impact, these multichannel measurements are constructed by recordings using a single receiver but from multiple impacts incrementally spaced from the receiver. Individual recordings are thus performed and the multichannel data records constructed. Crucial here is to synchronize the signals correctly in time. The data acquisition must therefore be triggered from the impact, either using a load cell in the hammer or possibly by e.g. an accelerometer attached at a fixed distance from the impact source in each recording.

Using MSOR the required amount of signals may be added to the multichannel data record. This is a convenient method to acquire large amount of data without buying expensive equipment with higher capacity, e.g. multiple accelerometers or large data acquisition devices. A disadvantage could be that it requires a repeatable trigger source. As two signals never will be identical (neither will the surrounding noise nor disturbances), there is always the risk that a differently triggered

recording could cause an incorrect phase shift between the individually recorded signals.

This method is used for the accelerometer measurements in Paper I but also for the study conducted in Paper V. In Paper I, where true multichannel measurements are compared to MSOR, the impact/-s and the receiver/-s switch place. A schematic of the MSOR setup is shown in Figure 14. The figure depicts the recording process where one single signal is recorded at a time using one impact source and one receiver. The impact source is then stepwise moved to record with increasing source-receiver distance.

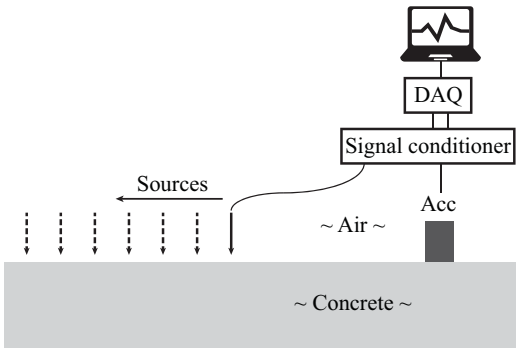

Figure 14: A multichannel simulation with one receiver setup. Multiple impacts are applied with increasing source-receiver distance. The data acquisition device is denoted DAQ.

The comparison of data records collected according to Sections 4.1.1 and 4.1.2 relies on the assumption of reciprocity; a signal from a point A to a point B is equal to a signal from B to A.

4.2 Data acquisition equipment

Two completely different data acquisition systems are used during the work of the papers given in the end of this thesis. These two systems will be further explained in Sections 4.2.1 and 4.2.2. For the study conducted in Paper IV, a microcontroller is employed to create automatic and repeatable impacts; this is explained in Section 4.2.3.

4.2.1 Condenser microphone array

A data acquisition trolley constructed by Ryden et al. (2008) is employed for the study conducted in Paper I. In this study, rolling non-contact surface measurements are compared to conventional stationary accelerometer measurements on a cement concrete slab. On the data acquisition trolley, seven audio microphones (ADK SC-1 condenser microphone with 10 mV/Pa sensitivity, ADK Microphones, Portland, OR, USA) are mounted as a straight array to simultaneously collect data from a single impact. The microphones are placed on the trolley with a constant spacing dx = 5 cm and the microphone tips ~20 mm above the surface, facing down. A small screw (~10 g) attached to a flexible metal stick is employed as the impact mechanism. The data acquisition is triggered from a piezo-ceramic element, epoxy glued on the top of the screw, creating an electrical current when the screw hits the slab surface. By rolling the trolley forward, the flexible metal stick is tensioned by a peg on the front wheel and a new impact is applied every 16 cm. Data are acquired from 60 positions along a straight survey line.

The data signals are collected from all seven microphones simultaneously on an eight channel data acquisition device (NI USB-6251, National Instruments, Austin, TX, USA) at a sampling frequency of 125 kHz. The eighth channel is used for the trigger (impact source).

All equipment on the data acquisition trolley is power supplied by a 12 V battery; the trolley is thus totally self supportive to enable large scale testing. The complete data acquisition trolley is shown in Figure 15 and also illustrated in the schematic in Figure 13.

The comparative accelerometer measurements are conducted using equivalent multichannel data records explained in Section 4.1.2. A single accelerometer (PCB model 356A15 with a 103.3 mV/g sensitivity, PCB Piezotronics, Depew, NY, USA) is employed in this study, collecting data from multiple impacts applied using the same impact source as in the rolling measurements. The data collection is sampled at the same sampling frequency and the signal is transmitted to the same data acquisition device as in the microphone measurements.

Figure 15: The data acquisition trolley employed in Paper I.

The two tested receiver types are shown to provide similar results regarding estimated V_R. However, the trolley and the data acquisition equipment have some shortcomings that motivate a new design. The rather bulky trolley makes the data collection sensitive to uncertainties; the long wheel base will cause misalignments between the uneven surface and straight bar holding the microphone array. A shorter wheel base could help the trolley follow the surface profile.

The number of channels available on the data acquisition device limits the number of signals that can be used. Only true multichannel measurements are possible when rolling measurements are performed. Hence, if a higher number of signals are required to provide high resolution results (see Section 3.3), an alternative data acquisition system is required.

The large dimensions and the high cost of the condenser microphones make them unfavorable. It is also difficult to mount them closer together than the 5 cm being used in Paper I. Smaller microphones mounted close together would allow measurements of shorter

wavelengths according to Nyquist-Shannon sampling theorem, stating that a minimum of two samples per wavelength are required to avoid spatial aliasing. This is even more important when measuring on asphalt concrete where the surface phase velocity is lower than in cement concrete.

Also, the impact source is not fully reliable. It occasionally fails for different reasons and the piezo-ceramic element (trigger) also needs to be replaced periodically. Because of this, there is a need to design a new data acquisition system.

Hereafter, this condenser microphone array system will be referred to as the old data acquisition system.

4.2.2 MEMS microphone array

After testing and evaluation, a new data acquisition system is designed and constructed in this project and is used to obtain measurements for Papers III and IV. The system contains a multichannel data acquisition device and an array of 48 air-coupled MEMS microphones (SPM0408LE5H, Knowles, Itasca, IL, USA). According to the manufacturer, this microphone type has a flat frequency response in the range 100 Hz – 10 kHz (Knowles, 2016); however, they operate at higher frequencies although the response sensitivity is not specified. In this project the exact physically calibrated amplitude is not important as long as the phase is consistent since it is only the phase information being used to estimate the phase velocities (see Section 3.3). The sensitivity is by the manufacturer given to be -18±3 dBV/Pa at 94 dB sound pressure level at 1 kHz.

The microphones have small dimensions that allow them to be mounted close together; in this case, they are mounted on a straight array with a constant spacing dx = 1.0 cm. Six individual circuit boards, each carrying eight microphones, are constructed and mounted tightly together (resulting in 48 microphones with a constant dx = 1.0 cm). Each circuit board is power supplied by two 1.5 V AA batteries. The data acquisition system uses 48 individual A/D converters in the form of six digitizer boards (NI PXI-5105, National Instruments), each board with simultaneously sampled channels. The digitizer boards are mounted in a chassis (NI PXI-1042, National Instruments) together with a controller unit (NI PXI-8106, National Instruments). Simultaneous sampling on all channels on all digitizer boards is achieved using the NI PXI-star trigger

bus. All data sampling is performed with 12-bit vertical resolution and ±1 V dynamic range with a frequency of 300 kHz for 20 ms.

Figure 16: (a) All equipment needed to perform surface wave testing using the MEMS data acquisition system. (b) Close-up photo of a circuit board holding 8 MEMS microphones. An AA battery is shown as size reference.

The data acquisition device is power supplied using a 12 V car battery via an inverter, transforming 12 V DC to 230 V AC.

In the study conducted in Paper III, the testing is performed using the data acquisition system in Figure 16(a) in a stationary manner. However, to achieve rolling continuous measurement along a survey line using the MEMS measuring system for Paper IV, all equipment needed to perform the testing is placed on a bicycle trailer, designed for this purpose, to enable full mobility. The trailer is displayed in Figure 17. The MEMS microphone array is attached underneath the trailer fairly close to the asphalt pavement so that the microphones' acoustic ports are located 37 mm above the surface. The array is also slightly rotated along its longitudinal axis to avoid multiple reflections between the pavement surface and the flat circuit board.

A third (supporting) wheel is mounted on the trailer to keep the microphone array and the trailer perfectly horizontal in order to avoid misalignment problems (Papers I and II).

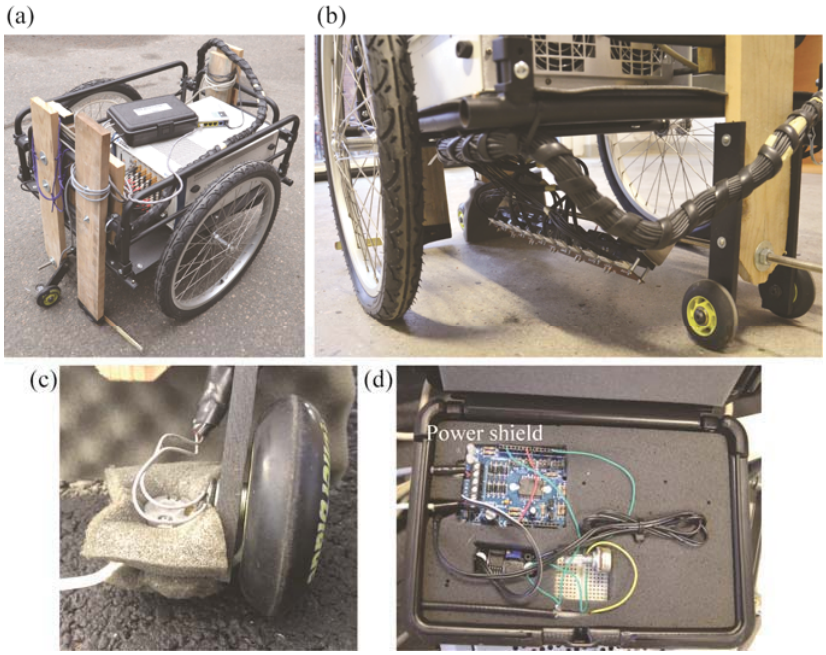

Figure 17: (a) The complete data acquisition system placed on the trailer employed for the rolling measurements and (b) a closer photo showing the microphone array's position underneath the trailer. (c) The seismic source embedded in soft foam attached to the arm hanging from the trailer. (d) All electronics employed to generate the impulses for the impact source. Note that the microcontroller itself is connected to the bottom side of the power shield and is not visible in the figure.

From here, the presented MEMS measuring system, rolling or stationary, is referred to as the new data acquisition system.

4.2.3 Automated impact

Due to the shortcomings of the old data acquisition system's impact source, a new automatic source is constructed for the study conducted in Paper IV. A solenoid, ejecting a small pin with approximate dimensions 4 mm×1.5 mm is employed as the actual source. The solenoid is embedded in soft foam (displayed in Figure 17) in order to suppress the sound wave generated due to the impact. It is further attached to a loose

arm, hanging from the data acquisition trailer described in Section 4.2.2. Also attached to the arm is a rubber wheel so that the solenoid pin (when not ejected) can be kept at a constant distance both above the surface (~2 mm) and from the first sensing microphone (150 mm) to create similar impacts for each measurement.

A microcontroller (Arduino Uno, Arduino, Somerville, MA, USA), having two functions is connected to the data acquisition system. First, switching the power on to eject the solenoid pin, and second, to trigger the data collection. Using the microcontroller, continuously repetitive electrical impulses can be created and sent to the solenoid. Together with the microcontroller, a so called power shield (VMA03, Velleman Modules, Gavere, Belgium) is employed to power the solenoid at higher voltage. The microcontroller and power shield are power supplied from the same 12 V battery as for the data acquisition device (see Section 4.2.2) using a series of adapters and inverters. Using the microcontroller, a 4 ms long impulse can be generated going from zero to its max, 24 V, from one sample to another, i.e. the data collection is started at the exact same time in relation to the ejection of the solenoid pin, for each measurement. Simultaneously, the same impulse is led directly to trigger the data acquisition via a potentiometer (to fit the voltage to the dynamic range of the data acquisition device). The microcontroller is directly connected to one of the data acquisition system's channels; hence, one microphone needs to be disconnected and the microphone array is slightly reduced to 47 microphones.

The complete electrical unit including the microcontroller and power shield is embedded in soft foam and placed in a hard case box to protect it from external elements (see Figure 17).

5 Results

The research presented in this thesis aims at determining the stiffness and thickness of layered structures. While Papers I, III, and IV are focused on stiffness estimation of a cement concrete slab (I) and the stiff top asphalt concrete layer (III and IV), Paper V introduces an alternative method to determine the thickness of a cement concrete slab. In Paper II, a simulation is intended to verify and further explore the results from Paper I.

Results from rolling surface wave measurements using the old air-coupled data acquisition system are compared to stationary accelerometer measurements in Paper I. The results are limited to the Rayleigh wave velocity estimation since its square is proportional to the real part of the complex modulus (storage modulus) *E'* according to Equations 5-7. Multichannel data records are collected from 60 positions along a survey line on a free cement concrete slab with a constant spacing = 16 cm, creating a measurement set. Multiple measurement sets are recorded to verify good repeatability. In Figure 18, five measurement sets collected with the microphone array are plotted and demonstrate very good repeatability. The microphone array length 0.30 m is indicated using the horizontal markers.

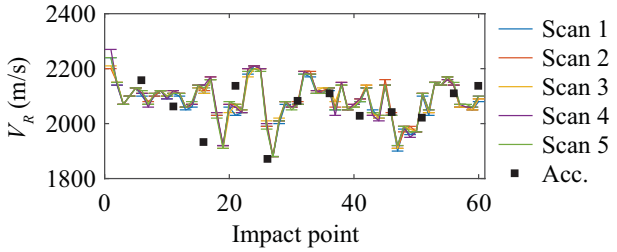

Figure 18: Evaluated Rayleigh wave velocities (V_R) from rolling surface wave measurements. Five separate microphone sets (1-5) are compared to 12 individual accelerometer measurements.

However, the evaluated Rayleigh wave velocity varies significantly along the survey line and differs slightly from the accelerometer measurement results (12 positions marked with squares in Figure 18). At closer inspection, the surface profile is found to be slightly uneven along

the survey line which can cause phase shifts in the air and subsequently inaccurate phase velocities to be evaluated. Similar measurements are therefore performed in the opposite direction in an attempt to even out microphone measurement errors according to Paper II. Surface wave measurements are also performed in the backward direction multiple times, after which the evaluated Rayleigh wave velocities from all measurement sets (five forward and five backward sets) are averaged along the synchronized x-axis and plotted in Figure 19.

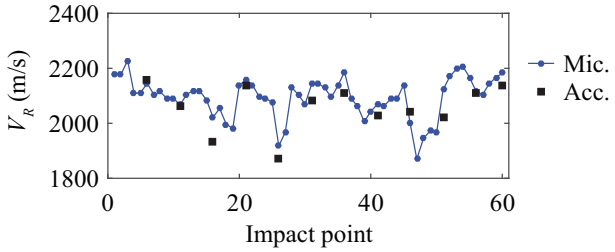

Figure 19: Evaluated Rayleigh wave results from microphone measurements performed in two opposite directions are averaged and compared to stationary accelerometer measurement results.

The comparison shows an improved fit between microphone (60 positions) and accelerometer (12 positions, independent of surface unevenness) measurements and the surface unevenness is hence believed to partly cause the scattered results.

It should be emphasized that the non-contact testing using air-coupled microphones are true multichannel measurements, thus multiple microphones collecting data simultaneously. These results are compared to multichannel simulations with one receiver where a single accelerometer collects data from multiple impacts. This difference in measuring techniques can possibly also explain some of the differences in the results.

To further investigate the potential problem of a misalignment between the pavement surface and the microphone array, measurements over a 20 m long, uneven surface corresponding to a high quality pavement (Andren, 2005; Bogsjö et al., 2012) are simulated. A small portion of this simulated surface profile is plotted in Figure 20. A perfectly horizontal array of air-coupled microphones is simulated above

the surface. Different numbers of receiving sensors and different array lengths are tested. The theoretical extra distances between the uneven surface and the microphones cause small time shifts for respective signal in the simulated data record in Figure 21(a), where a reference phase velocity of 2000 m/s is applied. In the figure, two simulated multichannel data records are plotted: one for a perfectly aligned microphone array plotted in gray in the background, and the second corresponding to a horizontal array above an uneven surface. Performing the summation of amplitudes for the two data records according to Figure 12, it can be seen in Figure 21(b) that the peak phase velocity is shifted. It should also be noted that the peak corresponding to the misaligned microphones is slightly lower since the 2000 m/s slope in time domain does not fit the same phase for each signal.

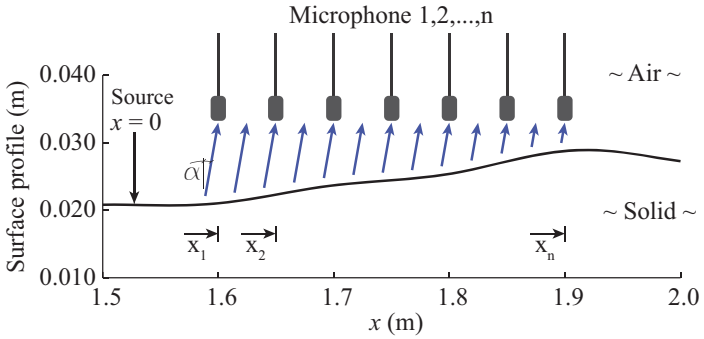

Figure 20: A small portion of the simulated uneven surface is plotted. The unequal distance from the surface to each microphone causes a time shift in the data record.

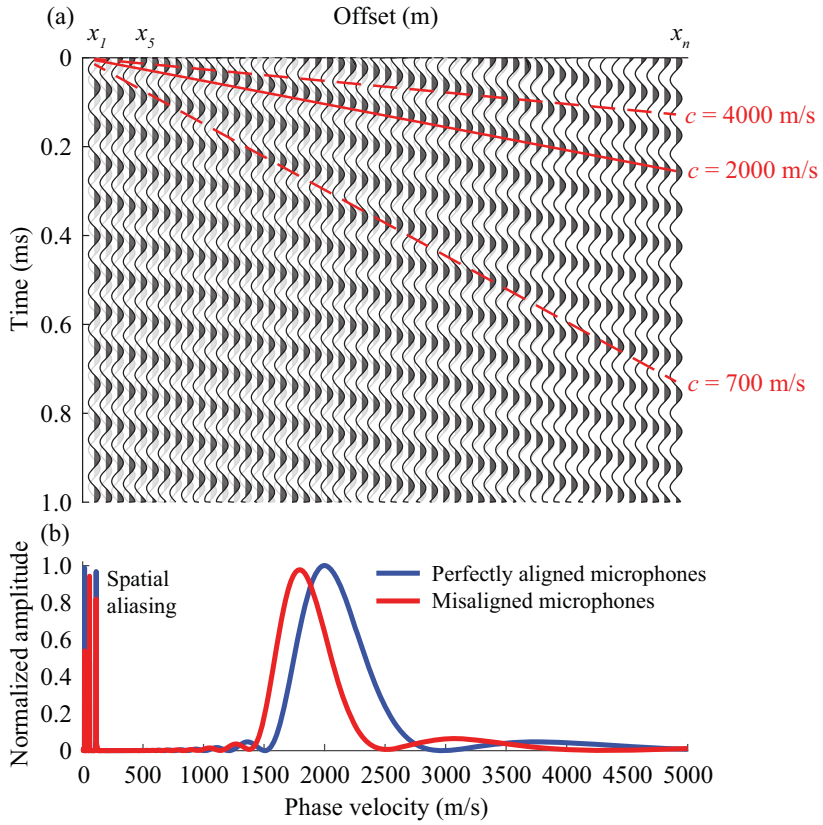

Figure 21: **(a) Simulated multichannel data record for a surface wave velocity of 2000 m/s and (b) the summation of amplitudes corresponding to a wide phase velocity range.**

This phase velocity shift is calculated for every new position of the simulated microphone array along the 20 m long uneven surface. The measured error is dependent on the surface wave velocity, due to the change in travel time ratio between solid and air. Calculated relative errors are plotted along with the surface profile in Figure 22.

The method of obtaining surface wave measurements in two opposite directions (forward and backward) in order to even out the measurement errors that are presented in Paper I, is also applied in this theoretical simulation to investigate if the method can work for a realistic surface

profile with non-linear irregularities. The relative errors calculated for a simulated microphone array rolling in two opposite directions are plotted on a synchronized x-axis in Figure 23. It can be seen that the calculated error curve from the backward roll is almost a reflection of the forward roll. The calculated mean of these two curves indicates almost zero errors along the surface.

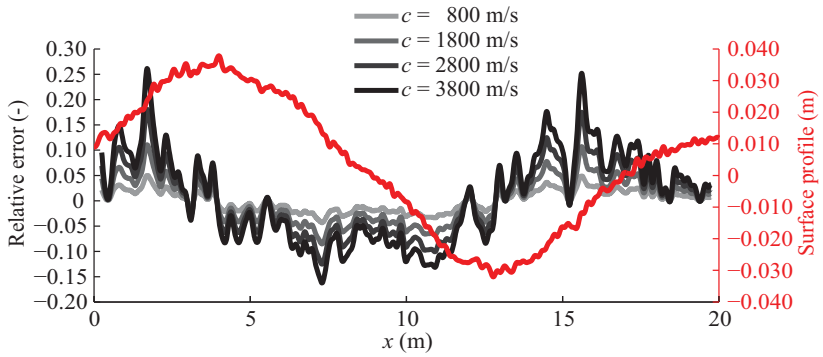

Figure 22: Calculated relative errors for difference surface wave velocities plotted against the left hand axis. The surface profile over which the simulation is performed is plotted against the right hand axis.

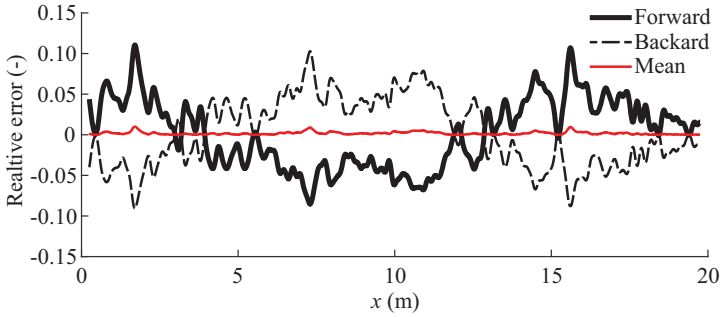

Figure 23: Relative calculation errors for the simulated rolling surface wave measurements performed in two opposite directions. The two calculation error curves almost reflect each other and the calculated mean indicates near zero errors.

The same effect as the rolling testing in two opposite direction would be given by attaching two impact sources on the measuring vehicle, one on each side of the microphone array. One impact could be applied by each of the two sources almost instantly, thus obtaining two multichannel measurements from the same position. This way, measurements from two opposite directions could be obtained along the survey line from a single roll.

A new field data acquisition system is introduced in Paper III, and surface wave data are collected from asphalt concrete pavements using 48 small MEMS microphones simultaneously. Five different test sections of a newly built highway are examined: a reference section designed with conventional asphalt mixtures (denoted “Ref.”), a conventional asphalt concrete section but with reduced thickness (P1), a stiffer asphalt concrete section (P2), and lastly two polymer modified bitumen sections (4.0% and 7.5% polymers in P3 and P4, respectively). After the field measurements are performed, cores are extracted from the in situ test locations and tested using impact resonance testing (Gudmarsson et al., 2012) to allow a direct comparison between the two methods. Using seismic laboratory testing, the core samples are characterized over wide temperature and frequency ranges and subsequently compared to the real part of the moduli extracted from the field measurements.

Multichannel data records are collected from single impacts and are demonstrated to provide robust results. Using the MASW method, the acquired surface wave data from ten multichannel data records are stacked and normalized in frequency domain according to Figure 24. The stacked frequency domain data are analyzed in a narrow range of wavelengths corresponding to near-surface (top asphalt layer) surface waves, illustrated with the red filled area in Figure 24. The phase velocity of the surface wave at every frequency is marked in green and can be seen to be dispersive. The Rayleigh wave velocity is assigned this phase velocity within the red wedge, see Figure 24.

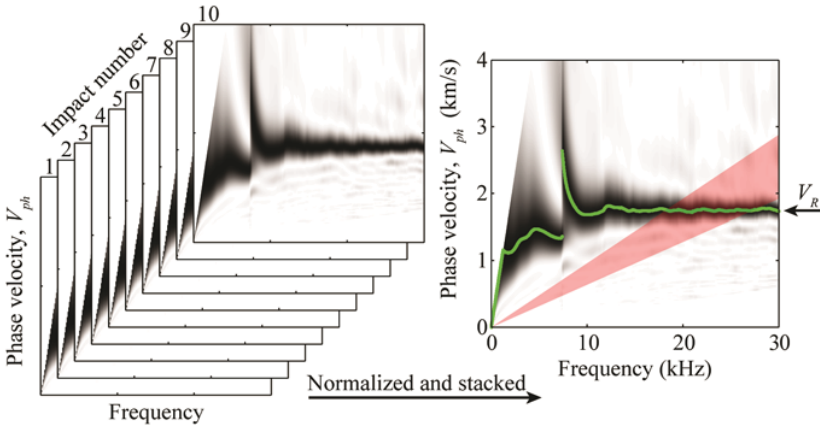

Figure 24: Frequency domain data from ten individual impacts are stacked and normalized. The Rayleigh wave velocity (V_R) is assigned the phase velocity value from the analyzed wavelength range (red wedge).

Using viscoelastic theory, the Rayleigh wave velocities enable estimations of the real part of the dynamic moduli. Comparisons of elastic moduli *E'* from field and laboratory measurement are plotted for the five different test sections in Figure 25. The comparative results demonstrate small differences (0.5-6.4%) at the in situ temperature and similar frequency. A limited number of tests are presented in Paper III; however, multiple field tests are performed in the same positions with high degree of repeatability. The tests are also performed at relatively high temperatures (18.1-26.7ºC) and at high frequencies (~20kHz) which implicate large attenuations.

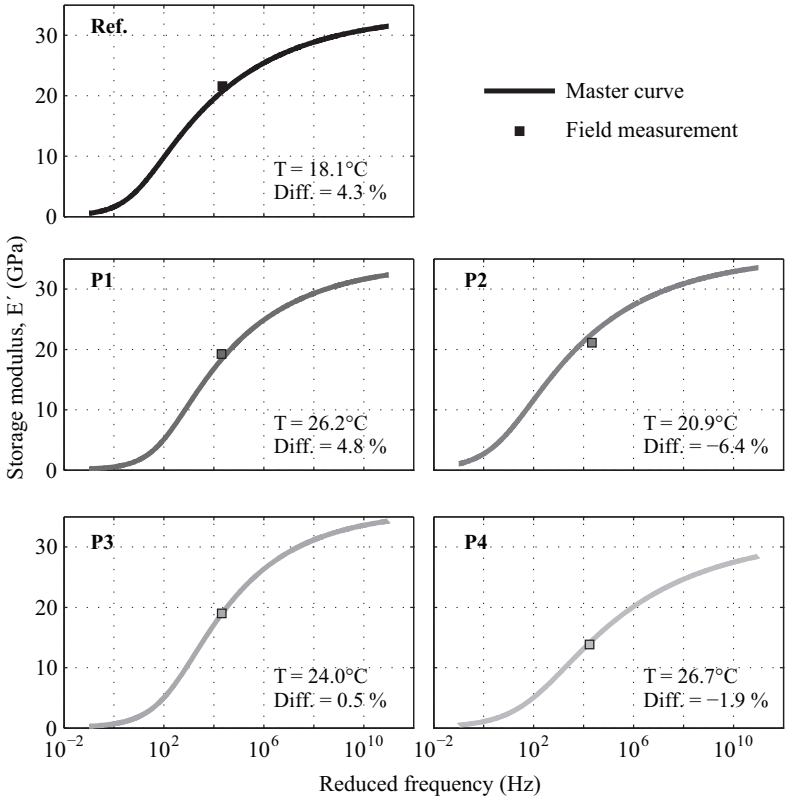

Figure 25: Comparative results from seismic laboratory (master curve) and in situ (squares) testing for the five tested pavement sections.

The very limited discrepancies between master curve and field measurement results in Figure 24 indicate that it should be possibly to apply the proposed non-contact field test method to quality control of asphalt pavements.

The data acquisition system introduced in Paper III is also employed in Paper IV. However, the focus in Paper IV is to enable rolling surface wave measurements using the air-coupled MEMS microphones. Extensive work is performed to design and build the data acquisition trailer presented in Section 4.2.2. By pushing the trailer at constant speed, 80 measurements are obtained along a straight survey line and form a measurement set. Multiple measurements sets are collected along

the same survey line in order to test if the data acquisition system is able to reproduce results multiple times and capture the strong temperature dependency of asphalt concrete.

Data are acquired on all microphones simultaneously, creating a multichannel data record, and analyzed in a similar manner as in the prior papers. An optimization routine, fitting a theoretical A_0 dispersion curve (Figure 8) to collected data in frequency domain, is written in Matlab (Mathworks, Natick, MA, USA) to extract the shear wave velocity. Assumed nominal asphalt concrete thickness of 45 mm and $\nu = 0.30$ are fixed in the optimization routine. The dispersion curve fitting is performed at a limited frequency range of 10-20 kHz for all test results at all temperatures. Most measurements generate an almost continuous dispersion curve, fitting the A_0 Lamb mode well as shown in Figure 26.

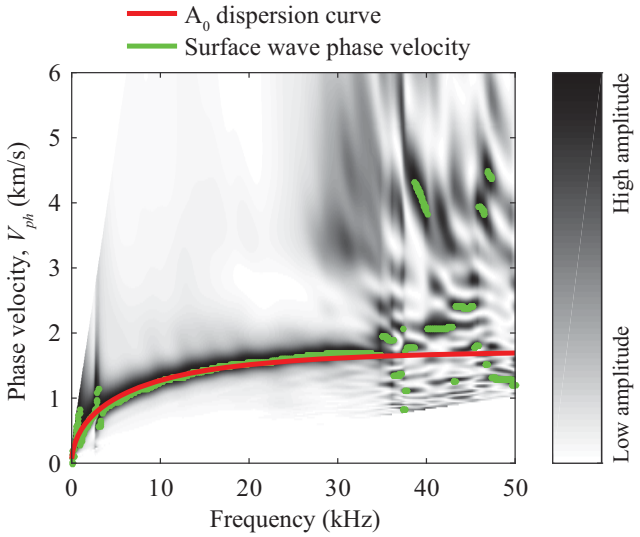

Figure 26: The theoretical fundamental antisymmetrical Lamb mode is fitted to measurement data in frequency domain in order to extract the shear wave velocity.

The shear wave velocity is determined automatically and objectively from each individual measurement along the survey line to receive a shear wave velocity profile, plotted against the left hand y-axes in

Figure 27. As can be seen in Figure 27, tests are performed at three different approximate temperature ranges (surface temperature). At the low range temperatures, plotted in Figure 27(a), the test results are highly repeatable and the shear wave velocity profile varies smoothly. These results indicate that the presented data acquisition system and analysis routine are robust. Measurement results from the midrange temperatures plotted in Figure 27(b) demonstrate, consistent with theory, a lower shear wave velocity compared to the low temperatures. Observe that the y-axes in Figure 27 all span a total range of 500 m/s but at different shear wave velocities. From ~1.2 m, the three shear wave velocities are also almost equal even at these higher temperatures. However, between the beginning of the survey line and up until ~1.2 m, there seems to be a small but systematic difference between the three velocity profiles. A possible explanation for this discrepancy could be that the asphalt concrete layer could be a little thicker in this end of the line, causing a lingering temperature gradient, affecting the results.

Extracted shear wave velocities from measurements performed at the higher temperatures, plotted in Figure 27(c), are generally lower compared to the two lower temperature ranges. The results are more scattered at these high temperatures.

More thoroughly examined results indicate that this could depend on the difficulty to set proper trigger values and limits in the post-processing of the data at higher temperatures. A requirement for future large scale testing to be effective is to enable setting these values. However, this is possible at the low and midrange temperatures. The generally robust results are considered to be promising. All tests are performed on a thin asphalt concrete layer (45 mm) and at relatively high temperatures. Waves propagating at these high temperatures, and the high frequencies required at such thin layers, are exposed to high attenuations. This setting can therefore be considered as a challenging setting for non-contact seismic testing. A thicker asphalt concrete layer and/or lower temperature should be easier to test since a higher signal to noise ratio is expected.

When fitting the A_0 dispersion curve to the experimental data, a cumulative error is calculated of the absolute phase velocity difference between the theoretical dispersion curve and assessed phase velocity in the specified frequency range 10-20kHz. All cumulative phase velocity errors are normalized against the maximum error in the nine

measurement sets. The curve fit factor is plotted with dashed lines against the right side y-axes in Figure 27, where the value 1.0 corresponds to a perfect fit and 0 corresponds to a poor fit.

Neither the frequency spectra from the microphones (see Impact Echo in Section 3.4) nor the backward propagating wave (Section 2.2.2) are able to detect the thickness resonance frequency so the layer thickness cannot be evaluated. However, it is noted that the thickness resonance can be expected to be ~34 kHz if approximate value of the layer thickness, V_P, and, ν are assumed. Unfortunately, this frequency is about the same as when spatial aliasing from the sound wave can be expected. Thus, it cannot be excluded that a backward propagating wave can be detected from a thicker asphalt concrete layer.

The large amount of data used for this study, is rapidly acquired (four minutes per scanned line) using the data acquisition trailer. This is an absolute requirement to enable large scale testing of pavements. The good consistency of the results in Figure 27 (especially at the lower and midrange temperature in Figure 27(a) and (b)) indicates good repeatability regarding the extracted shear wave velocity. Also, the results are able to capture the expected strong temperature dependency of asphalt concrete.

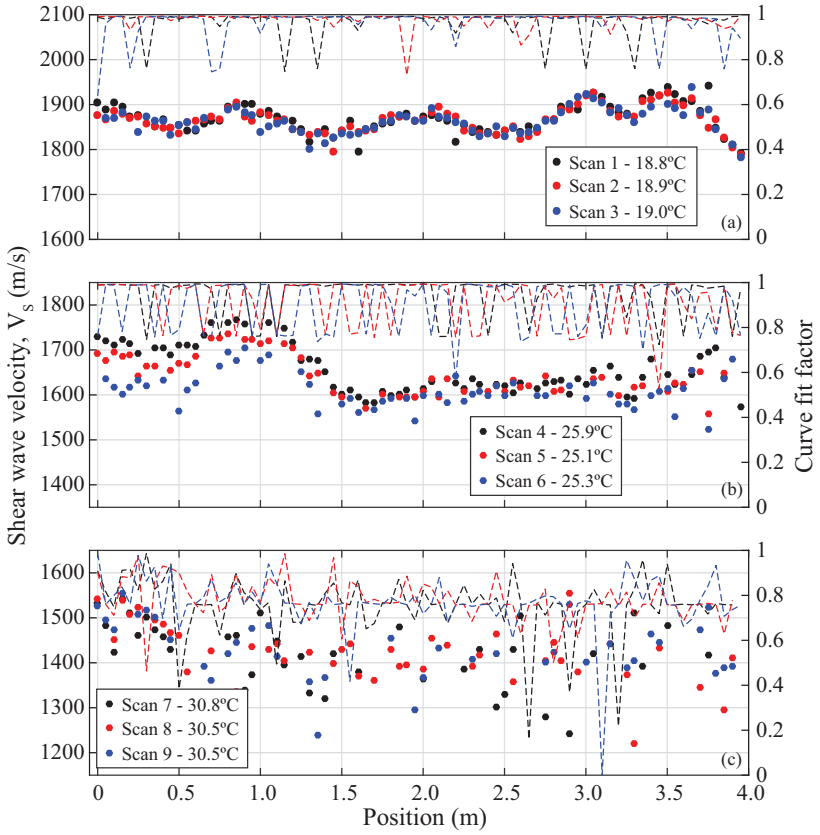

Figure 27: Extracted shear wave velocities from all surface wave tests performed along the survey line are plotted against the left hand y-axes. The tests are performed in three approximate temperature ranges: (a) low, (b) mid, and (c) high. Along with the assessed velocities, the curve fit factor is plotted with dashed lines against the right hand y-axes in corresponding colors.

All measurements presented in Papers I, III, and IV indicate that it is difficult to estimate the slab thickness using only the A_0 dispersion curve. The evaluated microphone results are not able to identify the thickness resonance frequency (IE frequency). In an attempt to overcome these difficulties, a novel technique to detect the thickness resonance frequency of slabs is presented in Paper V. Due to low signal-to-noise ratio, it is

generally difficult to apply the IE method, where the thickness resonance frequency is detected as a peak in the frequency spectrum, using microphone receivers. In Figure 28, one accelerometer and two air-coupled microphones are plotted along with their amplitude spectrum from a single impact. The IE resonance frequency is here expected to be ~6 kHz.

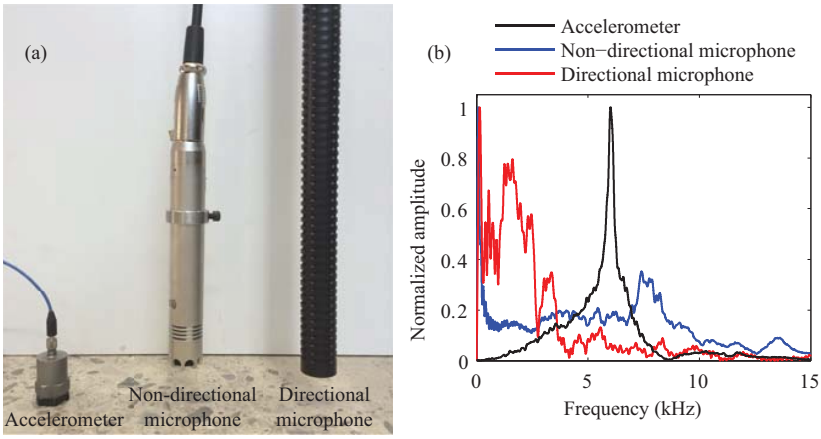

Figure 28: (a) Three tested receivers along with (b) their amplitude spectrum from a single impact.

The thickness resonance frequency is associated with the minimum frequency of the S_1 Lamb mode. However, by studying complex dispersion curves, it is shown that what appears to be the S_1 mode at low wave numbers actually is a branch of the S_2, propagating in the positive direction (positive group velocity) but with a negative phase velocity (see Section 2.2.2). This point on the S_1 dispersion is often referred to as the $S_{1\text{-ZGV}}$ where the index ZGV represents “zero group velocity”. Tests are performed in Paper V demonstrating that both accelerometers and air-coupled microphones can be employed as receivers, using this alternative approach, to identify the thickness resonance frequency to ultimately determine the slab thickness. The introduced method is first studied using a FE model. In that model, a free plate is given the approximate properties of the tested cement concrete slab. Data extracted in a way that is similar to how the real measurements are obtained, are plotted in

Figure 29. It is shown that the resonance is visible already in time domain as high amplitude wave at offsets corresponding to the wavelength at the so called $S_{1\text{-}ZGV}$ point, in the simulation model (see Figure 29(a)). Transformed into frequency domain, the simulated data are shown to fit theoretical dispersion curves very well both for positive and negative phase velocities in Figure 29(b) and (c), respectively. By summation of amplitudes over the negative phase velocity spectrum, a clear peak

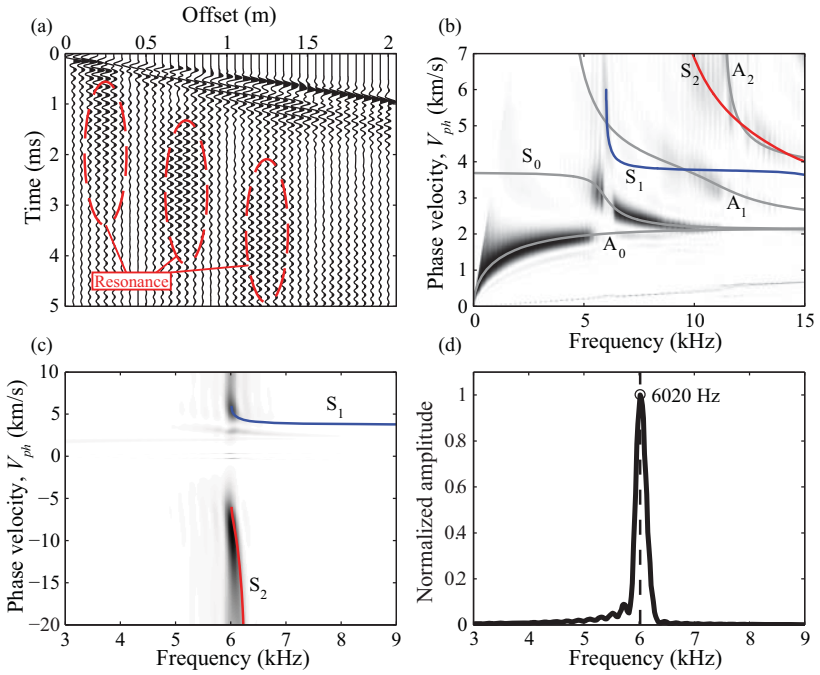

Figure 29: Extracted data from the FE model simulating the tested cement concrete slab. (a) A resonance phenomenon can be observed in time domain as high amplitude waves at offsets corresponding to the wavelength at the $S_{1\text{-}ZGV}$ point. (b) The data transformed into frequency domain fit the theoretical dispersion curves well. (c) Frequency domain data extracted at negative phase velocities show high amplitude wave in a narrow frequency range approximately corresponding to the S_2 Lamb mode. (d) Amplitudes summed over negative velocities reveal a clear peak frequency that corresponds very well with the theoretical thickness resonance frequency.

frequency can be detected close to the theoretical $S_{1\text{-}ZGV}$ frequency (6014 Hz) in Figure 29(d).

In situ tests are performed on a cement concrete slab using two different receivers. Data are collected using an accelerometer and analyzed in a similar way as the FE model. Note that only a single receiver is employed at once. Multichannel data records are constructed by applying multiple impacts at incremental offsets. This technique is referred to as the multichannel simulation with one receiver and is described in Section 4.1.2. This method is preferred over true multichannel measurements to enable collection of signals from a wide offset range.

The frequency domain data at negative phase velocities and the summation of amplitudes over this negative phase velocity range are plotted in Figure 30(a) and (b). According to theory, a distinct peak is identified equal to the theoretical thickness resonance frequency when the accelerometer is used. The same test and analysis are performed using an air-coupled microphone serving as a receiver. Evaluated data are plotted in Figure 30(c) and (d). In the summation of amplitudes in Figure 30(d), a peak is located at approximately the theoretical thickness resonance frequency. However, the amplitude summation is disturbed by multiple high amplitude peaks that are believed to originate from reflected acoustic waves and/or spatial aliasing. Lastly, in an attempt to suppress the negative influence of spatial aliasing and/or reflected acoustic waves, a small piece of soft foam is placed between the impact and the microphone. The same test and data analysis are performed once again and the results are plotted in Figure 30(e) and (f). It can be concluded that even a small and simple sound barrier as the piece of soft foam applied in this study, can significantly improve the signal-to-noise ratio. In the amplitude summation in Figure 30(f), a distinct peak is located at approximately the theoretically correct resonance frequency.

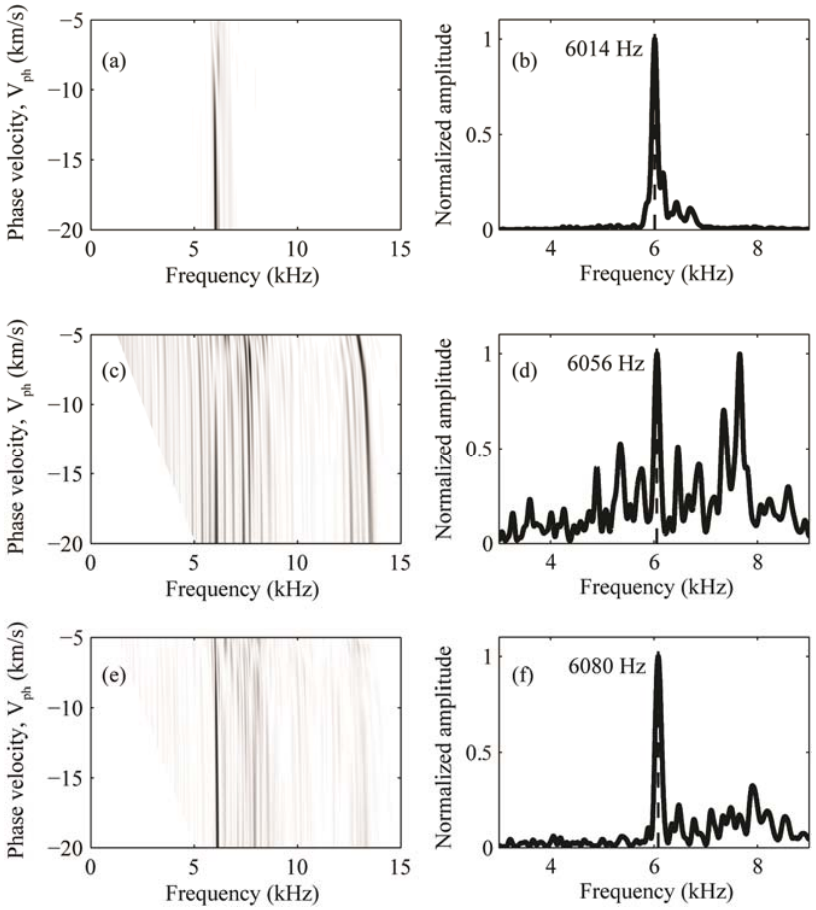

Figure 30: Frequency domain data at negative phase velocities collected using (a) accelerometer, (c) microphone, and finally (e) microphone with a sound barrier in front. Corresponding summations of amplitudes over the plotted phase velocity range (-20 - -5 km/s) are shown in (b), (d), and (f), respectively.

The introduced alternative to the IE method is observed to provide approximately the theoretical minimum frequency of the S_1 Lamb mode using both an accelerometer and a microphone as receivers. This demonstrates the possibility of obtaining measurements rapidly where

both stiffness and slab thickness can be determined from the same data record.

6 Summary of appended papers

This thesis is based on four journal papers and one conference paper. These papers are summarized in this chapter.

Paper I: Non-contact surface wave testing of pavements: comparing a rolling microphone array with accelerometer measurements

Rolling non-contact surface wave measurements performed using an array of seven air-coupled microphones is compared to conventional stationary accelerometer measurements. The compared results are limited to the Rayleigh wave velocity. It is shown that non-contact rolling measurements can provide a fast and reliable alternative to the more time-consuming accelerometer measurements. All measurements are performed on the same cement concrete slab. However, the results indicate that the measured Rayleigh wave velocity is sensitive to surface unevenness. Measures to overcome this problem are discussed and demonstrated using both forward and backward rolling measurements. It is also shown that the rolling measurements are highly repeatable.

Paper II: Effect of surface unevenness on in situ measurements and theoretical simulation in non-contact surface wave measurements using a rolling microphone array

Effects of a misalignment between a pavement surface and an air-coupled microphone array are investigated to assess the sensitivity to such imperfection at in situ surface wave measurements. A simulation is demonstrated where an array of non-contact sensors is rolled over an uneven, yet realistic, pavement. It is indicated that even small misalignments are capable of causing significant measurement errors. A method to overcome this problem is also presented, it is demonstrated how surface wave testing performed in two opposite directions generate two almost equally large measurement errors but with opposite signs. Simulations thus indicate that rolling testing in opposite directions could even out measurement errors to receive an approximate zero sum.

Paper III: Field and laboratory stress-wave measurements of asphalt concrete

Non-contact surface wave measurements on the top asphalt layer in a newly built pavement structure are performed in the field. A data acquisition system consisting of 48 micro-electro-mechanical system (MEMS) sensors is constructed for this study and employed to collect data. Core samples are then extracted from the field measurement locations and examined in the laboratory to enable comparison between the two. The laboratory measurements are performed in a range of temperatures and frequencies, which are then shifted around a chosen reference temperature to construct a master curve over a wide frequency range. The field and laboratory measurement results are compared at the field temperatures, demonstrating small differences. Furthermore, ten individual measurements are performed in the same location to verify good repeatability.

Paper IV: Non-contact rolling surface wave measurements of asphalt concrete

Rolling surface wave measurements are performed on an asphalt pavement to evaluate the shear wave velocity along a straight 4 m survey line. The multichannel data acquisition system presented in Paper III is mounted on a trailer designed for rapid field data acquisition. An automatic impact source is also designed, triggering the data collection at equal spacing by pushing the trailer at constant speed. A microcontroller is applied to create identical impact pulses.

Multiple sets of data are collected, each containing 80 individual multichannel measurements at specified positions with a constant spacing. Shear wave velocity (directly related to the real part of the dynamic modulus) is evaluated from each individual multichannel data record. Multiple tests are also performed at different temperatures to demonstrate the strong temperature dependency of asphalt concrete. Results show a high degree of repeatability at lower temperatures but with more noise and variation at higher temperatures (>30°C).

Paper V: Detecting the thickness mode frequency in a concrete plate using backward wave propagation

Impact Echo is an established method to determine the slab thickness by identifying the high amplitude peak, related to the thickness resonance, in a measured frequency spectrum from one receiver. It is a convenient method when an accelerometer is used as receiver while microphones often give too low signal-to-noise ratio. An alternative method to estimate the thickness resonance frequency is presented in this paper. By studying complex dispersion curves it is shown that the resonance is caused by two waves with counter-directed phase velocities at the resonance frequency. Using an array of receivers, it is demonstrated how propagating waves with a negative phase velocity can be measured in a narrow frequency range near the high amplitude resonance. The paper shows how the introduced negative phase velocity technique is able to provide results equivalent to the theoretically correct frequency. The discrepancies are considered to be insignificant.

7 Conclusions

Nondestructive surface wave testing of asphalt pavements has until today been based on stationary accelerometer testing. To enable faster quality control of pavements compared to what is possible today, measurements need to be obtained from asphalt concrete while rolling.

Non-contact surface wave measurements using an array of seven air-coupled microphones as receivers, are demonstrated to be able to provide surface wave velocity results similar to those from conventional accelerometer signals. However, it is crucial that the microphone array is in perfect alignment with the pavement surface to avoid any measurement errors.

A method to reduce the measurement errors due to misalignments is presented. Simulations show that it is theoretically possible to nearly eliminate the measurement errors due to misalignment, by performing rolling testing in two opposite directions.

Based on initial results obtained using the array with seven microphones, a new data acquisition system with 48 air-coupled MEMS microphones is designed and built. The high number of sensors creates a robust system that is able to provide high resolution results. Dynamic modulus of the top asphalt concrete layer from a newly built pavement, determined in the field, is compared to results from seismic laboratory testing of core samples, extracted from the field measurement positions. Multiple sections with different asphalt mixtures are tested and only minor discrepancies are demonstrated.

To realize rapid rolling testing, the new, fully automated data acquisition system is mounted on a trailer constructed for this purpose. Tests are performed by rolling at moderate speed. Evaluated data from multiple measurement sets are demonstrated to provide repeatable shear wave velocity values (stiffness) as well as capture the strong temperature dependency of asphalt concrete.

Rolling surface wave testing is performed on a thin single asphalt concrete layer and at relatively high temperatures. Despite challenging conditions, the fully automated measuring trailer is able to provide reliable results.

Results obtained using air-coupled microphones indicate that the stiffness of the top asphalt concrete layer can be characterized, while the

thickness is more difficult to evaluate. An innovative alternative method, based on Lamb waves with counter-directed phase velocity and group velocity, is presented. Negative phase velocities constitute a unique property only held by certain Lamb modes in a narrow frequency range. As opposed to conventional IE measurements where thickness determination is shown to be difficult to achieve using a microphone, this novel technique is demonstrated to provide acceptable thickness resonance frequencies using both an accelerometer and a microphone.

8 Recommendations for future work

The work presented in this thesis is based on surface wave testing conducted on a limited number of structures. More structures need to be tested and at different temperatures to fully validate the results presented here. Tests performed on a known structure in an environment where the temperature can be monitored or optimally controlled would be ideal. The effects of a temperature gradient through the asphalt concrete at various layer thicknesses are also recommended to be further studied.

Full characterization of the viscoelastic behavior of the asphalt concrete to assess the complex modulus requires the evaluation of surface wave attenuation as a function of frequency. Well calibrated amplitude measurements are then needed; however, this part was omitted from this project due to the amount of work with the equipment assembly and data processing. This would be an interesting parameter to include in future studies for a full comparison to the complex modulus assessed in the laboratory.

Slab thickness estimation using Lamb waves with counter-directed phase velocity and group velocity needs to be further explored. Tests should be performed on slabs of different asphalt mixtures and with different thicknesses. Also, in Paper V, a long microphone array with a high number of signals is employed to collect data. An investigation of length on the air-coupled receiver array and number of sensors required to detect the negative phase velocity waves would be of interest.

Ultimately the dynamic moduli and layer thicknesses could be determined for a multilayered structure. However, this requires an inversion of a vertical shear wave velocity profile and additional data processing.

Finally, some practical issues remain. This project involves non-contact surface wave testing performed while rolling at moderate walking speeds; however, increasing the test speed is desirable.

The use of a non-contact transmitting source is believed to be preferable. When a mechanical impact is employed, the contact time of the impact source in the ground could be a potential problem with increasing rolling speeds. However, it appears to be a challenging task due to the large contrast in impedance between air and asphalt concrete.

Lastly, the need for a proper positioning system increases with the area over which the tests are performed. Mapping the position for each performed test along with a surface temperature reading would be valuable for true large scale testing.

References

Abraham, O, Piwakowski, B., Villain, G., and Durand, O. (2012). Non-contact, automated surface wave measurements for the mechanical characterisation of concrete, *Constr. Build. Mater.*, 37, 904-915.

Achenbach, J.D. (1998). Lamb waves as thickness vibrations superimposed on a membrane carrier waves, *J. Acoust. Soc. Am.*, 103 (5), 2283-2286.

Airey, G.D., Rahimzadeh, B., and Collop, A.C. (2003). Viscoelastic linearity limits for bituminous materials, *Mater. Struct.*, 36 (10), 643-647.

Al-Hunaidi, M. (1992). Difficulties with phase spectrum unwrapping in spectral analysis of surface waves nondestructive testing of pavements, *Can. Geotech. J.*, 29 (3), 506-511.

Al-Qadi, I., Leng, Z., Lahouar, S., and Beck, J. (2010). In-place hot-mix asphalt density estimation using ground-penetrating radar, *Transp. Res. Rec.*, 2152, 19-27.

Al-Qadi, I., Ghodgaonkar, D., Varada, V., and Varadan, V. (1991). Effect of moisture on asphaltic concrete at microwave frequencies, *IEEE Trans. Geosci. Remote Sens.*, 29 (5), 710-717.

Ambrozinski, L., Piwakowski, B., Stepinski, T., and Uhl, T. (2014). Evaluation of dispersion characteristics of multimodal guided waves using slant stack transform, *NDT&E Int.*, 68, 88-97.

American Association of State Highway and Transportation Officials (AASHTO) (2007). Standard method of test for determining dynamic modulus of hot-mix-asphalt (HMA), AASHTO Designation: TP 62, Washington.

Andren, P. (2005). Power spectral density approximations of longitudinal road profiles, *Int. J. Veh. Des.*, 40 (1-3), 2-14.

Aouad, M.F., Stokoe, K.H., and Roesset, J.M. (1993). Evaluation of flexible pavements and subgrades using the spectral-analysis-of-surface-waves-method, University of Texas, Center for Transportation Research (CTR), Issue Number: 1175-7F, 383 p.

Bergmann, L., Hatfield, H., (1938). Ultrasonics and their scientific and technical applications. New York, John Wiley and Sons, Inc.

Bernard, S., Grimal, Q., and Laugier, P. (2014). Resonant ultrasound spectroscopy for viscoelastic characterization of anisotropic attenuative solid materials, *J. Acoust. Soc. Am.*, 135 (5), 2601-2613.

Blindow, N., Eisenburger, D., Illich, B., Petzold, H., and Richter, T. (2007). Ground penetrating radar, in: Environmental Geology: Handbook of Field Methods and Case Studies, Springer Berlin Heidelberg, Berlin, pp. 283–335.

Bogsjö, K., Podgórski, K., and Rychlik, I. (2012). Models for road surface roughness, *Veh. Syst. Dyn.*, 50 (5), 725-747.

Castaings, M. and Cawley, P. (1996). The generation, propagation, and detection of Lamb waves in plates using air-coupled ultrasonic transducers, *J. Acoust. Soc. Am.*, 100 (5), 3070–3077.

Chekroun, M., Le Marrec, L., Abraham, O., Durand, O., and Villain, G. (2009). Analysis of coherent surface wave dispersion and attenuation for non-destructive testing of concrete, *Ultrasonics*, 49 (8), 743-751.

Dai, X., Zhu, J., Tsai, Y.-T., and Haberman, M.R. (2011). Use of parabolic reflector to amplify in-air signals generated during impact-echo testing, *J. Acoust. Soc. Am.*, 130 (4), EL167–EL172.

Di Benedetto, H., Partl, M.N., Francken, L., and De La Roche Saint André, C. (2001). Stiffness testing for bituminous mixtures. *Mater. Struct.*, 34 (2), 66–70.

Gibson, A. and Popovics, J. (2005). Lamb wave basis for Impact-Echo method analysis, *J. Eng. Mech*., 131 (4), 438–443.

Groschup, R. and Grosse, C.U. (2015). MEMS microphone array sensor for air-coupled Impact-Echo, *Sensors*, 15 (7), 14932–14945.

Gudmarsson, A., 2014. Resonance testing of asphalt concrete (Doctoral thesis). KTH Royal Institute of Technology, Stockholm, Sweden. ISBN: 978-91-87353-50-5

Gudmarsson, A., Ryden, N., and Birgisson, B. (2012). Characterizing the low strain modulus of asphalt concrete specimens through optimization of frequency response functions, *J. Acoust. Soc. Am.*, 132 (4), 2304-2312.

Ham, S., Song, H., Oelze, M.L., and Popovics, J.S. (2017). A contactless ultrasonic surface wave approach to characterize distributed cracking damage in concrete, *Ultrasonics*, 75, 46–57.

Heisey, J., Stokoe II, K.H., and Meyer, A. (1982). Moduli of pavement systems from spectral analysis of surface waves. Transp. Res. Rec., 852, 22-31.

Heukelom, W. and Foster, C.R. (1960). Dynamic testing of pavements, *J. Soil Mech. Found.*, Div. 86, 2368–2372.

Hiltunen, D.R. and Woods, R.D. (1990). Variables affecting the testing of pavements by the surface waves method, *Transp. Res. Rec.*, 1260, 42–52.

Hoar, R. and Stokoe, K.H. (1978). Generation and measurement of shear waves in situ, in: Dynamic Geotechnical Testing, Construction Collection., West Conshohocken, PA, ASTM International, 3–29.

Ioannides, A.M., Barenberg, E.J., and Lary, J.A. (1989). Interpretation of falling weight deflectometer results using principles of dimensional analysis, *Proceedings of the 4th International Conference on Concrete Pavement Design and Rehabilitation*, 231–247, 18-20 April, Purdue University, IN.

Jones, R. (1955). A vibration method for measuring the thickness of concrete road slabs in situ, *Mag. Concr. Res.*, 7 (2), 97–102.

Kee, S.-H., Oh, T., Popovics, J.S., Arndt, R.W. and Zhu, J. (2011). Nondestructive bridge deck testing with air-coupled impact-echo and infrared thermography, *J. Bridge Eng.*, 17 (6), 928–939.

Kee, S.-H. and Zhu, J. (2010). Using air-coupled sensors to determine the depth of a surface-breaking crack in concrete, *J. Acoust. Soc. Am.*, 127 (3), 1279–1287.

Knowles (2013). Product data sheet for SPM0408LE5H: "Amplified Zero-Height SiSonic™ Microphone With Enhanced RF Protection," revision D, retrieved from www.knowles.com 11 Nov. 2016.

Labs4u (2017). Product data sheet for AS-0120 AMPT-SPT: "AMPT/SPT Asphalt Mixture Performance Tester," retrieved from www.labs4u-construction.co.uk 11 Nov. 2016.

Lamb, H. (1917). On waves in an elastic plate, *Proc. R. Soc. Lond. Ser. A*, 93 (648), 114–128.

Luukkala, M., Heikkila, P. and Surakka, J. (1971). Plate wave resonance—a contactless test method, *Ultrasonics*, 9 (4), 201–208.

Mindlin, R. (1960). Waves and vibrations in isotropic, elastic plates, in: Structural Mechanics*, Proceedings of the first symposium on naval structural mechanics*, 199–232. Stanford University, 11-14 Aug. 1958, Pergamon press.

Nazarian, S., Stokoe II, K.H., and Hudson, W. (1983). Use of spectral analysis of surface waves method for determination of moduli and thicknesses of pavement systems. *Transp. Res. Rec.*, 930, 38–45.

Nazarian, S., Yuan, D. and Tandon, V. (1999). Structural field testing of flexible pavement layers with seismic methods for quality control, *Transp. Res. Rec.*, 1654, 50–60.

Nguyen, H.M, Pouget, S., Di Benedetto, H., and Sauzéat, C. (2009). Time-temperature superposition principle for bituminous mixtures, *Eur. J. Environ. Civ. Eng.*, 13 (9), 1095-1107.

Park, C., Miller, R., and Xia, J. (1998). Imaging dispersion curves of surface waves on multichannel record, in: *SEG Technical Program Expanded Abstracts 1998,* Society of Exploration Geophysicists, 1377–1380.

Park, C.B., Miller, R.D., and Xia, J. (1999). Multichannel analysis of surface waves, *Geophysics*, 64 (3), 800–808.

Piwakowski, B. and Safinowski, P. (2009). Non-destructive non-contact air-coupled concrete evaluation by an ultrasound automated device, presented at the *Non-Destructive Testing in Civil Engineering (NDT-CE)*, 30 June-3 July 2009, Nantes, France.

Rayleigh, Lord (1885). On waves propagated along the plane surface of an elastic solid, *Proc. Lond. Math. Soc.*, 17 (1), 4–11.

Richart, F.E., Hall, J.R. and Woods, R.D. (1970). Vibrations of soils and foundations, Prentice-Hall Inc., Englewood Cliffs, NJ.

Rix, G.J., Stokoe II, K.H. and Roesset, J.M. (1991). Experimental study of factors affecting the spectral-analysis-of-surface-waves method, University of Texas at Austin, Center for Transportation Research, Austin, TX, Issue number: 1123-5, 188 p.

Roesset, J.M., Chang, D.-W., Stokoe II, and Aouad, M. (1990). Modulus and thickness of the pavement surface layer from SASW tests, *Transp. Res. Rec.*, 1260, 55-63.

Ryden, N., Lowe, M.J., and Cawley, P. (2008). Non-contact surface wave scanning of pavements using a rolling microphone array, AIP Conference Proceedings, 975 (1), 1328-1332.

Ryden, N., Park, C.B., Ulriksen, P. and Miller, R.D. (2004). Multimodal approach to seismic pavement testing, *J. Geotech. Geoenvironmental Eng.*, 130 (6), 636–645.

Ryden, N., Park, C.B., Ulriksen, P., Miller, R.D., 2003. Lamb wave analysis for non-destructive testing of concrete plate structures, *Proceedings of the Symposium on the Application of Geophysics to Engineering and Environmental Problems (SAGEEP 2003)*, 6-10 April 2003, San Antonio, TX.

Ryden, N., Ulriksen, P., Park, C.B., Miller, R.D., Xia, J., and Ivanov, J. (2001). High frequency MASW for non-destructive testing of pavements—Accelerometer approach. *Proceedings of the Symposium on the Application of Geophysics to Engineering and Environmental Problems (SAGEEP 2001)*, 4-7 March 2001, Denver, CO.

Saarenketo, T. (1997). Using ground-penetrating radar and dielectric probe measurements in pavement density quality control. *Transp. Res. Rec.*, 1575, 34–41.

Saarenketo, T. and Scullion, T. (2000). Road evaluation with ground penetrating radar, *J. Appl. Geophys.*, 43 (2-4), 119–138.

Said, S. (1995). VTI särtryck, vol. 242, Swedish National Road and Transport Research Institute (VTI), Lecture at the Course on Bituminous Pavements: Materials, Design and Evaluation at Uleåborg, Finland, 25-28 April 1995.

Sansalone, M., and Carino, N.J. (1986). Impact-echo: a method for flaw detection in concrete using transient stress waves. Rep. No. NBSIR 86-3452, National Bureau of Standars, Gaithersburg, MD.

Schmitt, R.L., Rao, C., and Von Quintus, H.L. (2006). Non-nuclear density testing devices and systems to evaluate in-place asphalt pavement density, Series: WHRP 06-12, Wisconsin Highway Research Program, Madison, WI.

Shearer, P. (1999). Introduction to Seismology, Cambridge University Press, Cambridge, UK.

Simonetti, F. and Lowe, M. (2005). On the meaning of Lamb mode nonpropagating branches. *J. Acoust. Soc. Am.*, 118 (1), 186–192.

Tokimatsu, K., Tamura, S., and Kojima, H. (1992). Effects of multiple modes on Rayleigh wave dispersion characteristics, *J. Geotech. Eng.*, 118 (10), 1529–1543.

Tolstoy, I. and Usdin, E. (1957). Wave propagation in elastic plates: low and high mode dispersion. J. Acoust. Soc. Am., 29 (1), 37–42.

Trafikverket (2011). TRVKB 10 Bitumenbundna lager, Document ID: TDOK 2011:082, Trafikverket, Borlänge, Sweden.

van der Poel, C. (1951). Dynamic testing of road constructions, *J. Appl. Chem.*, 1 (7), 281–290.

Weldegiorgis, M.T. and Tarefder, R.A. (2014). Laboratory investigation of asphalt concrete dynamic modulus testing on the criteria of meeting linear viscoelastic requirements, *Road Mater. Pavement Des.*, 15 (3), 554–573.

Zhu, J. and Popovics, J. (2007). Imaging Concrete Structures Using Air-Coupled Impact-Echo, *J. Eng. Mech.*, 133 (6), 628–640.

Zhu, J. and Popovics, J. (2002). Non-contact detection of surface waves in concrete using an air-coupled sensor, AIP Conference Proceedings, 615 (1) 1261–1268.

Zhu, J. and Popovics, J.S. (2005). Non-contact imaging for surface-opening cracks in concrete with air-coupled sensors, *Mater. Struct.*, 38 (9), 801–806.